UNIVERSITAT POLITÈCNICA DE CATALUNYA
BARCELONATECH
Escola Superior d'Enginyeries Industrial, Aeroespacial i Audiovisual de Terrassa

Escola Tècnica Superior d'Enginyeria Industrial, Audiovisual i Aeroespacial de Terrassa - ESEIAAT

Bachelor's degree in Aerospace Technologies Engineering

Bachelor's degree thesis

Study and Design of the attitude control of a cubesat 1U based on reaction wheels

Report

Author: Paula Sorolla Bayod

Director: David González Diez

September 30, 2019

Contents

Acknowledgements **IX**

Glossary **XI**

Abstract **XIII**

Signed declaration **XV**

1 Introduction **1**

1.1 Motivation 1

1.2 Aim 1

1.3 Scope 2

1.4 Initial requirements and limitations 3

2 State of the art **5**

2.1 The Cubesat concept 5

2.2 Attitude Determination and Control system 6

2.2.1 Attitude Determination 6

2.2.2 Attitude Control 8

3 Mechanical model description **11**

3.1 Reference Systems 11

3.1.1 Earth Centred Inertial (ECI) Reference Frame - **i** 11

3.1.2 Earth Centered Earth Fixed (ECEF) Frame - **e** 12
3.1.3 Orbit Reference Frame - **o** 12
3.1.4 Body Reference Frame - **b** 12
3.2 Rotation matrix definition 13
3.3 Attitude representation 14
3.3.1 Euler angles 14
3.3.2 Quaternions 15
3.4 Moment of Inertia 17
3.5 Satellite Dynamics modeling 18

4 External Disturbance Torques **21**
4.1 Gravity gradient torque 22
4.2 Magnetic torque 23
4.3 Aerodynamic torque 24
4.4 Solar radiation 25
4.5 Total Disturbance 26

5 Attitude Control Model Design **29**
5.1 Reaction wheels configurations 29
5.1.1 Orthogonal 3-wheel configuration 30
5.1.2 Redundant 4-wheel configuration 31
5.1.3 Tetrahedral 4-wheel configuration 32
5.1.4 Off-centered 4-wheel configuration 34
5.2 DC Motor Model 35
5.3 Commercial Off-The-Shelf Reaction Wheels Assemblies 36
5.4 The reaction wheels saturation problem 38
5.4.1 Momentum damping 38
5.5 Simulink implementation 40

5.6 Simulink blocks 43

6 Simulation Results 47

6.1 3-wheel configuration 48

6.2 4-wheel Redundant configuration 50

6.3 4-wheel tetrahedric configuration 51

6.4 4-wheel Off-centered configuration 53

6.5 1-wheel failure 55

6.5.1 Redundant model failure 56

6.5.2 Off-centered model failure 57

6.5.3 Tetrahedric model failure 58

6.6 Comparison 59

7 Environmental impact assessment and economical costs 61

8 Conclusions 63

8.1 Next steps 64

List of Figures

1.1 The CubeSat Standard 3

2.1 CubeSats examples [3] 6
2.2 Attitude Determination Devices examples 7
2.3 Attitude Determination Devices examples 9

3.1 ECEF and ECI Reference Frames 12
3.2 Orbit and Body Reference Frames [6] 13
3.3 Roll-pitch-yaw Euler angles [7] 14

4.1 Disturbance torques for a CubeSat 27

5.1 Orthogonal 3-wheel configuration 30
5.2 Redundant 4-wheel configuration 31
5.3 Tetrahedron configuration of four reaction wheels 32
5.4 Tetrahedron configuration on $x_b - y_b$ and $x_b - z_b$ planes 33
5.5 Off-centered 4-wheel configuration 34
5.6 DC motor circuit [16] 35
5.7 Simulink model of the DC motor 36
5.8 Commercial Reaction Wheel 37
5.9 Commercial Reaction Wheel Assembly [19] 37
5.10 Magnetorquer actuators 39

5.11 Attitude Control System - Simulink model (3-wheels) 41
5.12 Attitude Control System - Simulink model (3-wheels) 42
5.13 Simulink model. Control block 43
5.14 Simulink model. Actuators block 44
5.15 Simulink model. Attitude dynamics block 45

6.1 Attitude control, 3-wheel configuration 48
6.2 Power consumption, 3-wheel configuration 49
6.3 Wheels angular velocity, 3-wheel configuration 49
6.4 Attitude control, 4-wheel Redundant configuration 50
6.5 Power consumption, 4-wheel Redundant configuration 51
6.6 Wheels angular velocity, 4-wheel Redundant configuration 51
6.7 Attitude control, 4-wheel tetrahedric configuration 52
6.8 Power consumption, 4-wheel tetrahedric configuration 52
6.9 Wheels angular velocity, 4-wheel Tetrahedric configuration 53
6.10 Attitude control, 4-wheel Off-centered configuration 53
6.11 Power consumption, 4-wheel Off-centered configuration 54
6.12 Wheels angular velocity, 4-wheel Off-centered configuration 54
6.13 Redundant model, extra wheel failure attitude response 56
6.14 Redundant model, z-axis wheel failure attitude response 57
6.15 Off-Centered model, wheel failure attitude response 58
6.16 Tetrahedric model, wheel failure attitude response 59

List of Tables

2.1 Attitude determination techniques summary [1] 7
2.2 Attitude control techniques summary [1] 9

4.1 Disturbance torques magnitude summary 26

5.1 Reaction Wheel commercial assemblies 37

6.1 Cubesat 1U parameteres 47
6.2 Reaction wheels and motor parameters 48
6.3 Defined manoeuvre for the normal-state simulations 48
6.4 Defined manoeuvre for the degraded-state simulations 55
6.5 Reaction wheels configurations performance comparison 59

7.1 Environmental impact assessment summary 61
7.2 Project's budget summary 62

Acknowledgements

Throughout the development of this Bachelor's Degree thesis, I have received a great deal of support and assistance. I would like to express my thanks to David Gonzalez for assessing and supporting the Thesis development.

Secondly, I would like to thank my family, for supporting me during this four years and teaching me new lessons every day. Thanks to my parents for giving me the opportunity to achieve a goal like this.

Finally, I would like to express my gratitude to all the professors who have thought me all the knowledge I have acquired in the degree. Thank you to all my classmates for sharing this journey with me and making the every day routine a little brighter.

Glossary

RW: Reaction Wheel

ACS : Attitude Control System

ADCS: Attitude Determination and Control System

COM: Center of Mass

DC: Direct Current

DOF: Degree of Freedom

ECEF: Earth Centered Earth Fixed

ECI: Earth Centered Inertial

PID: proportional–integral–derivative controller

IMU: Inertial Measurement Unit

I : moment of Inertia .... $[kg \cdot m^2]$

I_x : moment of Inertia about x $[kg \cdot m^2]$

SF : solar radiation constant ... $[W/m^2]$

p_{SR} : force of solar pressure .... $[N/m^2]$

F_{SR} : force due to solar radiation .. $[N]$

ρ : atmospheric density .... $[kg/m^3]$

A_{inc} : sat. area perpendicular to u_v $[m^2]$

ω : angular velocity .... $[rad/s]$

α : angular acceleration .... $[rad/s^2]$

u_v : unit vector in velocity direction

C_d : drag coefficient

c_{ps} : solar center of pressure

cg : center of gravity

c_{pa} : aerodynamic center of pressure

Abstract

On this thesis, the study and design of the attitude control of a cubesat 1U is performed.

The mechanical model definition and the space environment description are used to develop a Simulink model where reaction wheels are used as actuators for the Attitude Control.

Once the model is defined, a control algorithm taking into account external disturbances has been defined and simulated for different actuator configurations.

KEYWORDS
Attitude Control, CubeSat, Reaction Wheels,
Modeling, Simulink, Space Dynamics

Signed declaration

I declare that,

- the work in this Degree Thesis is completely my own work,
- no part of this Degree Thesis is taken from other people's work without giving them credit,
- all references have been clearly cited,

I understand that an infringement of this declaration leaves me subject to the foreseen disciplinary actions by The Universitat Politècnica de Catalunya - BarcelonaTECH. Paula Sorolla Bayod,

Terrassa, September 30, 2019

Chapter 1

Introduction

1.1 Motivation

The aerospace industry is continuously evolving, and one of the most recent solutions has been presented in terms of CubeSats. The first six CubeSats were launched on June 2003 and its popularity has only grown.

CubeSats are considered as a technology testbed and an affordable means to enter the prestigious space technology development field. However, there are still some unfixed design challenges and that makes them a perfect area of study.

Attitude control is necessary for the proper functioning of any satellite. Actuators used for satellite attitude control include reaction wheels, magnetorquers, thrusters, etc. In order to design a system capable to orient a satellite, space mechanics need to be applied.

1.2 Aim

The aim of this Degree Thesis is the design and study of an Attitude Control System based on reaction wheels to be implemented on a CubeSat 1U.

The CubeSat mathematical model is defined in Simulink software in order to simulate an attitude control algorithm using reaction wheels as actuators.

The implementation of different reaction wheels configurations on the model is used to determine the optimal performance in different modes of operation.

1.3 Scope

In this thesis, the modelling and the simulation of the attitude control system for a CubeSat 1U is taken into consideration. As mentioned in the Aim section, it has been developed using Matlab and Simulink software.

A fist extensive bibliographic research regarding and Attitude Determination and Control Systems for CubeSats has been done in order to develop a model that fits COTS technology.

As part of the scope of this project, the mechanical model of the system has been determined, sized and modelled in Simulink. To do so, the environmental space of the spacecraft has been also studied in terms of disturbance torques applied externally to the CubeSat.

Different solutions and configurations for the ADCS have been proposed and simulated using a control algorithm also implemented using Simulink software. The Satellite attitude towards certain manoeuvres, static-state and detumbling have been analysed.

Other tasks not specified above are out of the scope of this Thesis, such as the determination of the disturbance torques change in the time or its direction, as the worst-case has been always taken.

1.4 Initial requirements and limitations

The Attitude Control System is to be developed using Reaction Wheels as actuators.

Moreover, the most important limitation comes in terms of volume and weight as it is designed for a one-unit CubeSat. The CubeSat standard specifies dimensions and launching weights of the satellite to being a 10cm side cube with a maximum mass of $1,3\ kg$.

An example of the structure that hosts all the CubeSat components is presented in figure 1.1a, a typical system distribution inside a CubeSat 1U can be seen in figure 1.1b. The examples below make clear the limitations of the system's design.

A typical weight for the ADCS system is $10-15\ \%$ of the total weight of the satellite [1], which would result in an approximate weight of $200\ g$ for the whole system.

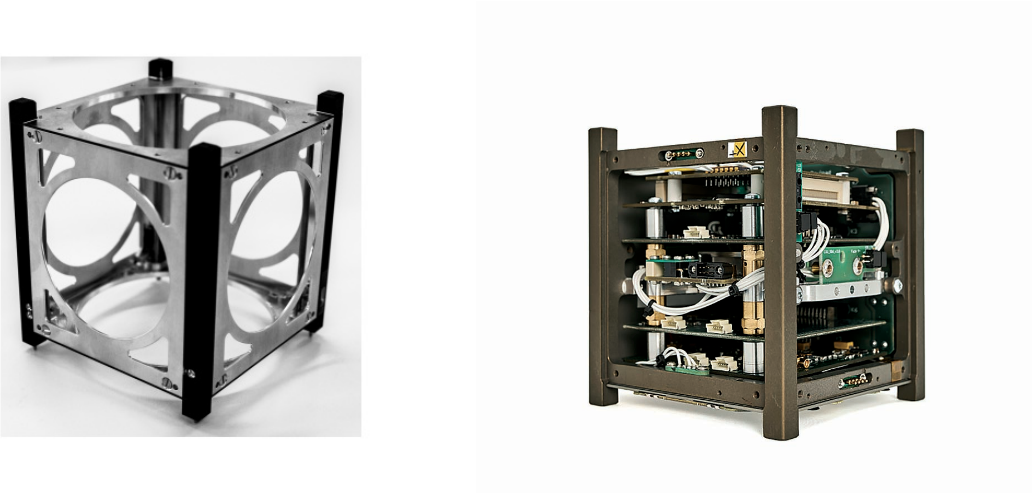

(a) CubeSat 1U Structure

(b) CELESTA CubeSat, CERN educational project

Figure 1.1: The CubeSat Standard

No requirements of attitude accuracy or response-time are previously set. Nevertheless, an optimal performance of these variables will be pursued while preserving the CubeSat Standard constraints.

Chapter 2

State of the art

On this chapter, different current solutions and results for attitude control systems used in satellites are explained and summarised. With this current ADCS studies, the reaction-wheel system solution is justified.

2.1 The Cubesat concept

The CubeSat results in a picosatellite standard which design was proposed by professors Jordi Puig-Suari of California Polytechnic State University and Bob Twiggs of Stanford University in 1999.

A CubeSat is a small satellite in the shape of a 10 cm cube and a mass up to $1,3$ kilograms [2]. With this simple design, they have become very popular because of being small, cheap and efficient. With an estimated budget of $90.000\$ - 120.000\$$ CubeSats can be made and launched, becoming an 'affordable' option for schools and universities across the world. Between 40 and 50 universities around the world were developing Cubesats in 2004. Figure 2.1 shows different examples of some launched CubeSats.

The first CubeSats launched in June 2003 on a Russian Eurockot, and approximately 75 CubeSats had entered orbit by 2012. [4]

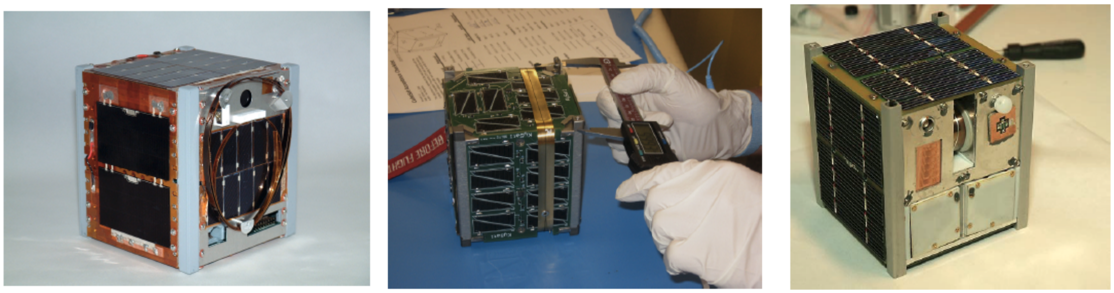

(a) Tokyo (Japan) (b) Kentucky (US) (c) Norway Space Center

Figure 2.1: CubeSats examples [3]

2.2 Attitude Determination and Control system

The attitude of a satellite refers to the angular orientation and stabilisation of a defined body-fixed coordinate frame with respect to a separately defined external frame in space, despite the external disturbing forces acting on it [5]. This requires the vehicle attitude determination with the use of sensors, and the vehicle control with the use of actuators.

2.2.1 Attitude Determination

In the spacecraft attitude determination, the actual spacecraft orientation is estimated from measurements. Some of the sensors that have been used through the years and are still in use are:

GYROSCOPES - Gyroscopes are composed of spinning wheels in the axis on which the rotation is to be measured. As they are relative attitude sensors, they require a known initial value and inaccurate measurements can drift to a significant error.

MAGNETOMETERS - Magnetometers sense magnetic field strengths and direction. The measurements are compared to the Earth's magnetic field map (which is dependent on the spacecraft position) to determine the attitude. Moreover, it can only be used at low altitude orbits, where the magnetic field is strong enough.

SUN SENSORS - Sun sensors sense the direction of the Sun, commonly based on some solar cells and shades that can determine the Sun's position.

HORIZON SCANNERS - Horizon scanners are optical instruments that determine the 'limb' of the Earth's atmosphere often using thermal infrared sensing.

STAR TRACKERS - Star trackers are also optical instruments that determine the position of stars using cameras or photocells. The attitude is determined relative to the position of the surrounding detected stars (see Figure 2.2).

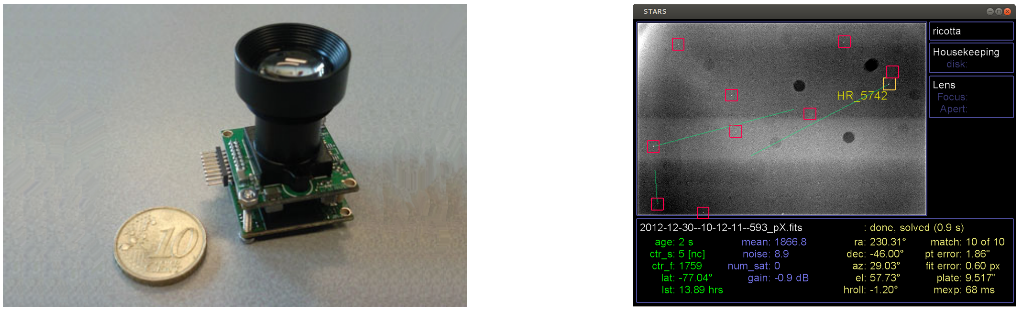

```
2012-12-30--10-12-11--593_pX.fits              : done, solved (0.9 s)
     age: 2 s          mean: 1866.8          ra: 230.31°      match: 10 of 10
   ctr_s: 5 [nc]      noise: 8.9            dec: -46.00°    pt error: 1.86"
   ctr_f: 1759      num_sat: 0               az: 29.03°    fit error: 0.60 px
     lat: -77.04°      gain: -0.9 dB         el: 57.73°        plate: 9.517"
     lst: 13.89 hrs                       hroll: -1.20°         mexp: 68 ms
```

(a) CubeSat star tracker

(b) EBEX 2012 star tracker software

Figure 2.2: Attitude Determination Devices examples

SUMMARY

Method	**Accuracy (°)**	**Performance Remarks**
Gyroscope	$0.01/h$	Best short-term reference, costly
Sun Sensor	$0.001 - 0.1$	Simple, reliable, cheap, intermittent use
Horizon scanner	$0.02 - 0.03$	Expensive, orbit-dependent, poor in yaw
Magnetometer	1	Cheap, low altitude use, continuous coverage
Star tracker	0.001	Expensive, heavy, complex, high accuracy

Table 2.1: Attitude determination techniques summary [1]

It is typical to use optical sensors in CubeSats, as new technologies allow these sensors to be very accurate in a reduced dimension and weight components as the star tracker presented in figure 2.2.

2.2.2 Attitude Control

Attitude control implies a process, usually occurring more or less continuously, of returning the spacecraft to a desired orientation, given that the measured attitude reveals a discrepancy with respect to the desired attitude.

PASSIVE ATTITUDE CONTROL

Passive stabilisation techniques take advantage of basic physical principles and naturally occurring forces by designing the spacecraft to enhance the effect of one while reducing the others [1]. In effect, disturbance torques explained in future section 4 are used to control the spacecraft.

An advantage of passive control is the ability to attain a very long satellite lifetime but against disadvantages of passive control are relatively poor overall accuracy.

SPIN STABILISATION - Spin stabilisation techniques are commonly combined with thrusters. The gyroscopic action of the rotating aircraft mass is used as the stabilizing mechanism.

GRAVITY-GRADIENT STABILISATION - Gravity-gradient stabilisation is based on the restoring torque that the gravitational Earth's field produces towards the higher primary inertia axis of the satellite as explained in section 4.1 (See Figure 2.3).

ACTIVE ATTITUDE CONTROL

The basic concept of active attitude control is that the satellite attitude is measured and compared with a desired value. The error signal is then used to determine a corrective torque manoeuvre T_C, which is implemented by the on-board actuators. The control principle is further explained in section 5.5

REACTION JETS - At least two thrusters acting on each of the satellite axes coupled, will provide a torque capable to orient the spacecraft.

MAGNETIC TORQUERS - Magnetic torquers provide a moment against the magnetic Earth's field when a controlled electrical current is provided to the coil.

CONTROL MOMENT GYROS - A control moment gyro consists of a spinning rotor (reaction wheel) and one or more motorised gimbals that tilt the rotor's angular momentum (See Figure 2.3).

REACTION WHEELS - Reaction wheels are provided with an electric motor and provide very precise attitude determination on the axis they are acting.

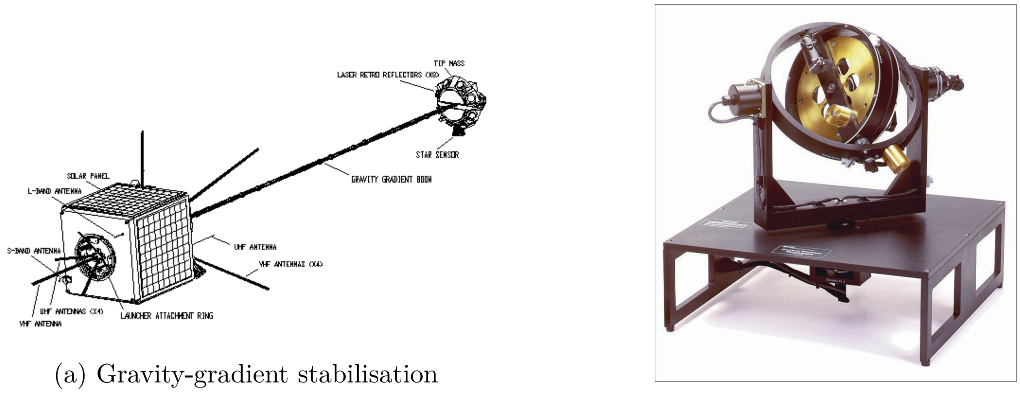
TIP MASS
LASER RETRO REFLECTORS (X8)
STAR SENSOR
GRAVITY GRADIENT BOOM
SOLAR PANEL
L-BAND ANTENNA
UHF ANTENNA
VHF ANTENNAS (X4)
S-BAND ANTENNA
UHF ANTENNAS (X4)
LAUNCHER ATTACHMENT RING
VHF ANTENNA

(a) Gravity-gradient stabilisation

(b) Control moment gyro

Figure 2.3: Attitude Determination Devices examples

SUMMARY

Table 2.2 summarises the different methods of spacecraft control explained above

Method	**Accuracy (°)**	**Performance Remarks**
Spin stabilization	0.1	Passive, simple, low cost, inertially oriented
Gravity gradient	$1-3$	Passive, simple, low cost, central-body oriented
Reaction jets	0.1	Quick, high authority, costly, consumables
Magnetic torquers	$1-2$	Near-Earth usage, slow, lightweight, low cost
Control moment gyros	0.1	High authority, quick, heavy, costly
Reaction wheels	0.01	Quick, costly, high precision

Table 2.2: Attitude control techniques summary [1]

Most common attitude control devices used in CubeSats are passive and rotational active controls, such as gravity-gradient or reaction wheels and magnetorquers.

Chapter 3

Mechanical model description

On a first stage of the project, the Mechanical model of the Satellite is to be determined in order to understand the Attitude Control requirements.

Reference systems, rotation matrixes and attitude representation methods are to be clear to finally present the satellite dynamic equations that apply the reaction wheel attitude control system in study.

3.1 Reference Systems

Fist step in order to analyse and design an Attitude Control System is to define the coordinate reference systems to work with. A satellite's attitude is convenient to be described as a deviation relative to a chosen reference frame.

3.1.1 Earth Centred Inertial (ECI) Reference Frame - i

This frame is fixed in space, thus it is a non-accelerated reference frame that allows Newton's Laws application. The origin is located at the center of the Earth.

Z-axis points towards the North Pole, X-axis points towards Vernal Equinox and Y-axis points complete the right hand Cartesian coordinate system (see Figure 3.1).

3.1.2 Earth Centered Earth Fixed (ECEF) Frame - e

ECEF frame's origin is also located at the center of the Earth, however X and Y axes rotate with the Earth relative to the ECI frame about the Z-axis.

X-axis points towards the intersection of Greenwich meridian and the Equator. Y-axis completes the right-handed orthogonal system (see Figure 3.1).

The ECEF frame rotates relative to the ECI frame with a constant angular velocity of $w = 7.2921 \cdot 10^{-5}\ rad/s$

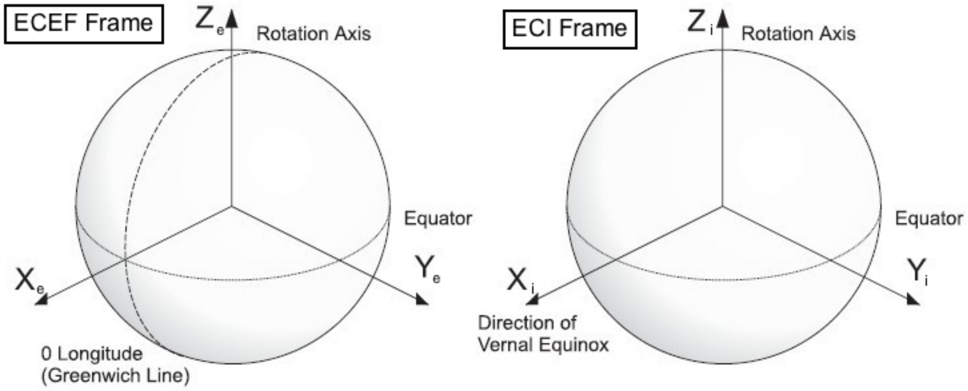
ECEF Frame
Z_e
Rotation Axis
Equator
X_e
Y_e
0 Longitude
(Greenwich Line)
ECI Frame
Z_i
Rotation Axis
Equator
X_i
Y_i
Direction of
Vernal Equinox

Figure 3.1: ECEF and ECI Reference Frames

3.1.3 Orbit Reference Frame - o

The origin of this frame coincides with the Centre Of Mass (COM) of the satellite.

Z-axis points towards the center of the Earth. X-axis points in the velocity direction tangentially to the orbit. Y-axis completes the right-hand system (see Figure 3.2).

3.1.4 Body Reference Frame - b

The body frame is fixed with the satellite and its origin is located again at the COM of the satellite. The orientation of the satellite is described relative to the orbit frame.

The nadir side of the satellite is in Z-axis direction, while X and Y-axes coincide with the orbit frame axes when the satellite has an attitude of 0 degrees in roll, pitch and yaw (see Figure 3.1).

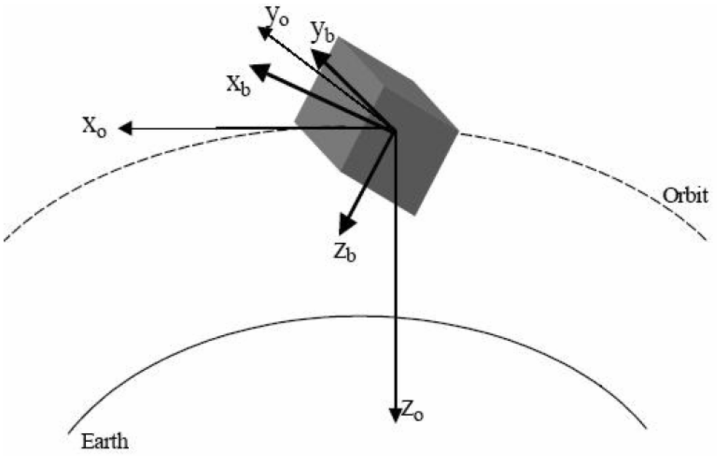

Figure 3.2: Orbit and Body Reference Frames [6]

3.2 Rotation matrix definition

A rotation matrix describes the orientation of a frame b with respect to a frame a [7]. It becomes useful to orient a satellite towards Earth direction-defined positions.

The rotation matrix is a 3 x 3 matrix with nine elements. The orthogonality of the matrix gives six constraints on the elements of the matrix so that there are only three independent parameters that describe the rotation matrix.

Rotation matrices have three statements [8]:

- Rotate vectors within a reference frame.
- Transform vectors represented in one reference frame to another.
- Describe the mutual orientation between two coordinate frames, where the column vectors are cosines of the angles between the two frames.

3.3 Attitude representation

There are many ways to represent the attitude of the satellite in a reference frame. But frequently *Euler angles* and *Quaternions* are used in many applications.

3.3.1 Euler angles

The attitude can be represented using roll (ϕ), pitch (θ) and yaw (ψ) angles. Those angles represent the rotations about the x, y and z axis in rotation from one frame to another. These angles are named Euler Angles: $\Theta = \begin{bmatrix} \phi \\ \theta \\ \psi \end{bmatrix}$

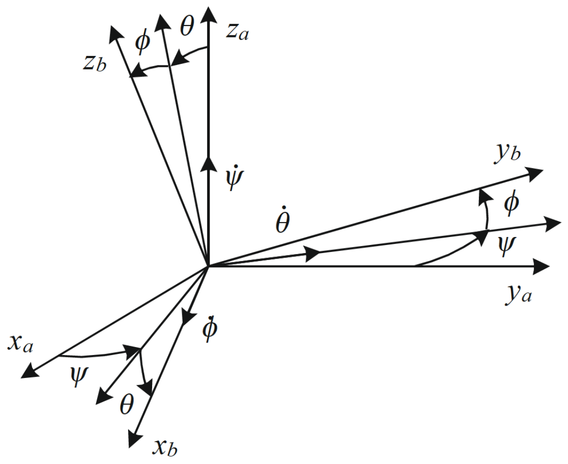

Figure 3.3: Roll-pitch-yaw Euler angles [7]

The rotation matrixes are expressed as follows:

$$R_{x,\phi} = \begin{bmatrix} 1 & 0 & 0 \\ 0 & cos\phi & -sin\phi \\ 0 & sin\phi & cos\phi \end{bmatrix} \quad R_{y,\theta} = \begin{bmatrix} cos\theta & 0 & sin\theta \\ 0 & 1 & 0 \\ -sin\theta & 0 & cos\theta \end{bmatrix} \quad R_{z,\psi} = \begin{bmatrix} cos\psi & -sin\psi & 0 \\ sin\psi & cos\psi & 0 \\ 0 & 0 & 1 \end{bmatrix} \tag{3.1}$$

Now, taking into account the reference systems described in 3.1, the rotation matrix

R_B^O is described by a rotation ψ (yaw) about the z-axis, then a rotation θ (pitch) about the y-axis and finally a rotation ϕ (roll) about the x-axis. This results:

$$R_B^O = R_z(\psi)\ R_y(\theta)\ R_x(\phi) = \begin{bmatrix} c\psi c\theta & -s\psi c\phi + c\psi s\theta s\phi & s\psi s\phi + c\psi c\phi s\theta \\ s\psi c\theta & c\psi c\phi + s\psi s\theta s\phi & -c\psi s\phi + s\psi c\phi s\theta \\ -s\theta & c\theta s\phi & c\theta c\phi \end{bmatrix} \tag{3.2}$$

3.3.2 Quaternions

First described by the Irish mathematician Sir William Rowan Hamilton in 1843, *quaternions* consist of a 4-tuple whose primary application is in a quaternion rotation operator. In this section, the equivalence and advantages of quaternions over the conventional rotation matrixes are presented [9].

Quaternions have 4 dimensions, 1 real and 3 imaginary, and are represented as:

$$\mathbf{q} = \begin{bmatrix} a \\ b\mathbf{i} \\ c\mathbf{j} \\ d\mathbf{k} \end{bmatrix} \tag{3.3}$$

The elements i, j and k satisfy the following relations:

$$i^2 = j^2 = k^2 = -1 \tag{3.4}$$

$$ij = -ji = k \qquad jk = -kj = i \qquad ki = -ik = j \tag{3.5}$$

As they have four parameters, one real part η and three imaginary parts ϵ, a rotation about a unit vector $(k_x,\ k_y,\ k_z)$ through an angle φ is represented as:

$$\eta = cos\frac{\varphi}{2} \quad , \qquad \eta = \begin{bmatrix} \epsilon_1 \\ \epsilon_2 \\ \epsilon_3 \end{bmatrix} = \begin{bmatrix} k_x\ sin(\varphi/2) \\ k_y\ sin(\varphi/2) \\ k_z\ sin(\varphi/2) \end{bmatrix} \quad , \qquad q = \begin{bmatrix} \eta \\ \epsilon_1 \\ \epsilon_2 \\ \epsilon_3 \end{bmatrix} \tag{3.6}$$

and represent a rotation about a unit vector $[k_x\ k_y\ k_z]$ through an angle φ. The unit quaternions satisfy $q^T q = 1$ which also means that $\eta^2 + \epsilon_1^2 + \epsilon_2^2 + \epsilon_3^2 = 1$

Finally, transformation from Euler angles to quaterions can be calculated as [6]:

$$q = \begin{bmatrix} \eta \\ \epsilon_1 \\ \epsilon_2 \\ \epsilon_3 \end{bmatrix} = \begin{bmatrix} c(\phi/2)c(\theta/2)c(\psi/2) + s(\phi/2)s(\theta/2)s(\psi/2) \\ s(\phi/2)c(\theta/2)c(\psi/2) - s(\phi/2)c(\theta/2)s(\psi/2) \\ c(\phi/2)s(\theta/2)c(\psi/2) + s(\phi/2)c(\theta/2)s(\psi/2) \\ c(\phi/2)c(\theta/2)s(\psi/2) - s(\phi/2)s(\theta/2)c(\psi/2) \end{bmatrix} \tag{3.7}$$

The transformation from quaternions to Euler angles can be expressed as [6]:

$$\begin{gathered} \phi = atan\left(2\left(q_2 q_3 + \eta q_1\right), \left(\eta^2 - q_1^2 - q_2^2 - q_3^2\right)\right) \\ \theta = asin\left(\left(q_1 q_3 - \eta q_2\right)\right) \\ \psi = atan\left(2\left(q_1 q_2 + \eta q_3\right), \left(\eta^2 + q_1^2 - q_2^2 - q_3^2\right)\right) \end{gathered} \tag{3.8}$$

And finally, the rotation matrix can be expressed in quaternions as [6]:

$$R_O^B(q) = R_{\eta,\epsilon} = 1_{3x3} + 2\eta S(\epsilon) + 2S^2(\epsilon) \tag{3.9}$$

3.4 Moment of Inertia

The moment of inertia denoted by I, measures the extent to which an object resists rotational acceleration about a particular axis:

$$I = \begin{bmatrix} I_{xx} & -I_{xy} & -I_{xz} \\ -I_{yx} & I_{yy} & -I_{yz} \\ -I_{zx} & -I_{zy} & I_{zz} \end{bmatrix} \tag{3.10}$$

Where I_x, I_y and I_z are the moments of inertia about the x_b, y_b and z_b axes and $I_{xy} = I_{yx}$, $I_{xz} = I_{zx}$ and $I_{yz} = I_{zy}$ are the products of inertia defined as follows::

$$\begin{aligned} I_{xx} &= \int (y^2 + z^2)\ dm & \qquad I_{xy} &= \int (xy)\ dm \\ I_{yy} &= \int (x^2 + z^2)\ dm & \qquad I_{xz} &= \int (xz)\ dm \\ I_{zz} &= \int (x^2 + y^2)\ dm & \qquad I_{yz} &= \int (yz)\ dm \end{aligned}$$

A uniform density cube will be assumed as the studied CubeSat. Then, with $d\ [m]$ side and mass $M\ [kg]$, the inertial matrix for a cube results as:

$$I = M\frac{d^2}{6} \begin{bmatrix} 1 & 0 & 0 \\ 0 & 1 & 0 \\ 0 & 0 & 1 \end{bmatrix} \tag{3.11}$$

Note that if the diagonal terms are much larger as non-diagonal, the uniform density assumption is not far from reality.

3.5 Satellite Dynamics modeling

In this section, the dynamics equations that apply the satellite in study will be presented using the Newton-Euler formulation in which the angular momentum changes related to applied torque.

Given the momentum p and the position vector r, the angular momentum h is:

$$h = r \times p \tag{3.12}$$

Then, if the angular momentum is derived using Newton's second law, having $v \times v = 0$ and $p = mv$ [6], one has:

$$\frac{\partial}{\partial t}h = \left(\frac{\partial}{\partial t}r \times p\right) + \left(r \times \frac{\partial}{\partial t}p\right) \quad = (v \times mv) + (r \times ma) \quad = r \times F = \tau \tag{3.13}$$

Where v is the velocity vector and τ is the total torque applied to the satellite.

Moreover, the angular momentum h can be also defined by the corresponding inertia matrix I, and the satellite angular velocity ω:

$$h = I\omega \tag{3.14}$$

Then, to start with our case of study, it is assumed that the satellite behaves as a **rigid solid with only reaction wheels control actuators**, then the total angular momentum is defined as:

$$H_B = I\omega_b + h_w \tag{3.15}$$

Where I states for the inertia matrix of the spacecraft, w_b is its angular velocity in the body frame and h_w is the angular momentum generated by the reaction wheels. In the following section 5, the reaction wheel distribution matrix T is presented, then for the 4-wheel configuration, the angular momentum h_w can be defined as:

$$h_w = TI_w\omega_w \tag{3.16}$$

where I_w is the reaction wheel diagonal inertia matrix defined in section 3.4 and ω_w is the angular speed of the 4 reaction wheels.f

Taking Euler's moment equations [1], we have:

$$\frac{d}{dt}H_b = -\omega_b(t) \times H_b(t) + T_d(t) \tag{3.17}$$

Where T_d is the total external disturbance torque that is defined in section 4.

Using equations 3.16 and 3.17:

$$\dot{H}_b = \left[\frac{dH}{dt}\right]_b = I\frac{d\omega_b}{dt} + h_w \tag{3.18}$$

$$I\frac{d\omega_b}{dt} = -\omega_b(t) \times (I\omega_b + h_w) + T_d(t) - h_w \tag{3.19}$$

By taking the principle of momentum exchange, we can say that the angular momentum produced by the reaction wheels is applied to the satellite with opposite sign. Then if we define T_C as the commanded torque:

$$\dot{h}_w = -T_C \tag{3.20}$$

$$\frac{d\omega_b}{dt} = I^{-1}\left[-\omega_b(t) \times (I\omega_b + h_w) + T_d(t) + T_C\right] \tag{3.21}$$

Chapter 4

External Disturbance Torques

Spacecraft orbiting are subject to numerous disturbance forces which, if not acting through the center of mass, result in a net torque being imported to the vehicle [1].

Assessment of these external disturbance torques is essential for the Attitude Control System design, hence, for the Reaction Wheel Assembly sizing.

The four main sources of disturbance torques from the environment in a LEO orbit are:

- Gravity gradient
- Aerodynamic
- Solar radiation
- Earth's magnetic field

The worst-case torque will be calculated for each case, all the calculations and equations have been extracted from the main reference [10], but also [11], [12] and [1] have been consulted.

4.1 Gravity gradient torque

Planetary gravitational fields decrease with distance r from the center of the planet according to the Newtonian $1/r^2$ law. Thus, a satellite in orbit will experience a stronger attraction on its 'lower' side than its 'upper' side [1]. This differential attraction results in a torque tending to rotate the satellite to align its minimum inertia matrix with the local vertical.

It is interesting to comment that the Gravity Gradient Stabilisation passive method described in section 2.2.2 is sustained by this principle.

The maximum Earth gravity gradient can be expressed as:

$$T_g = \frac{3\mu_\oplus}{2R^3}\ |I_z - I_y|\ sin(2\theta) \tag{4.1}$$

where:

T_g: is the maximum gravity torque
$\mu_\oplus$: is the Earth's gravitational parameter ($3.986\ 10^{14}\ m^3/s^2$)
R: is the orbit radius $(6.370 + 600)\ 10^3\ m$
θ: is the maximum deviation of the orbit frame Z-axis (see 3.1.3)
I_z, I_y: are the moments of inertia about z and y-axis

The value of θ represents the inclination in which the torque arm will act. Then $sin(2\theta) = 1$ is the worst-case value that it can take. Then solving 4.1 we get:

$$T_g = \frac{3 \times 3.986\ 10^{14}}{2 \times (6.970\ 10^3)^3}\ |0,0609 - 0,1052| \times 1 \tag{4.2}$$

$$\boxed{T_g = 7,8171\ 10^{-8}\ \ Nm}$$

4.2 Magnetic torque

The magnetic torque is the effect of the Earth magnetic field at low altitude orbits, and can be expressed as:

$$\bar{T}_m = \bar{m} \times \bar{B} \tag{4.3}$$

where:

T_m: is the magnetic torque
D: is the residual dipole of the CubeSat, that will be here estimated
B; is the Earth's magnetic field

The residual dipole due to current loops and residual magnetisation in the satellite can only be estimated experimentally with the satellite of study. Taking a look at the bibliography referenced for this chapter, values between $[0,2-20 \;\; A\ m^2]$ are proposed for satellites. Nevertheless, as the object of study is a CubeSat these values are not a good reference. Then, using as reference the case exposed by [13], a value of $0,01\ A\ m^2$ has been taken.

Then, the Earth's magnetic field can be expressed by:

$$B = \frac{2M}{R^3} = \frac{2 \times 7.96\ 10^{15}}{6.970\ 10^3} = 4,7016\ 10^{-5} \tag{4.4}$$

computed using the Earth's magnetic moment ($M = 7.96\ 10^{15} \;\; tesla\ m^3$) and the orbit radius $R = (6.370 + 600) \cdot 10^3\ m$ as follows:

Finally, the magnetic disturbance torque results:

$$T_m = 4,7016\ 10^{-5} \times 0,01 \tag{4.5}$$

$$\boxed{T_m = 4,7016\ 10^{-7} \;\; Nm}$$

4.3 Aerodynamic torque

Upper atmosphere density is responsible of a drag force applied to the satellites orbiting the Earth at low altitudes. This drag force will produce a disturbance torque on the spacecraft due to any offset existing between the aerodynamic center of pressure and the center of mass. This aerodynamic force is expressed as:

$$F_{aero} = \frac{1}{2}\ \rho\ V^2\ C_d\ A_{inc} \tag{4.6}$$

where:

ρ: is the atmospheric density at given altitude
V: is the spacecraft velocity also depending on the orbit altitude
C_d: is the drag coefficient. A reference value between $2-2,5$ is taken for CubeSat
A_{inc}; is the incident satellite surface area

At an orbit of $h = 600km$, using [11] the air density can be approximated as:

$$\rho \approx 3,725\ 10^{-12}\ kg/m^3$$

Also, the spacecraft velocity can be calculated as:

$$V = \sqrt{\frac{G\ M}{R}} = \sqrt{\frac{6,67\ 10^{-6} \times 5,97\ 10^{24}}{6.370\ 10^3 + 600\ 10^3}} = 7.558,5m/s \tag{4.7}$$

Assuming C_{pa} to be the center of pressure (CP) and cg the gravitational center, the aerodynamic torque is:

$$T = R_{cp} \times F_a \tag{4.8}$$

Thus, the worst-case aerodynamic torque has been calculated analogue as in section 4.4:

$$\tau_{aero} = F_{aero} \times (c_{pa} - cg) \tag{4.9}$$

$$\tau_{aero} = \frac{1}{2} \times 3,725\ 10^{-12} \times 7.558,5^2 \times 2,5 \times 0,1^2 \times (0.05 - 0) \tag{4.10}$$

$$\boxed{T_a = 1,3301\ 10^{-7}\ \ Nm}$$

4.4 Solar radiation

Solar radiation are photons that are drawn of the Sun under solar activity, its perturbation has more effect at high altitudes as being a function of distance from the Sun. It is common using the solar radiation constant SF which expresses the solar flux density [14]:

$$SF = 1.353\ W/m^2 \tag{4.11}$$

to calculate the force of solar pressure (p_{SR}) per unit area using the speed of light (c) :

$$p_{SR} = \frac{SF}{c} = \frac{1.353}{3\ 10^8} = 4,51\ 10^{-6}\ N/m^2 \tag{4.12}$$

Then, the force due to solar radiation [15] can be expressed as:

$$F_{SR} = -p_{SR}\ c_R\ A_S\ \ cos\ i \tag{4.13}$$

where:

C_R: is the reflectivity coefficient, that can be also expressed with the reflectance factor q as: $C_R = (1+q)$. From [15] we get a typical value of $q = 0.6$ for satellites
A_S: is the satellite surface area
i is the angle of incidence of the sun to the satellite surface

Finally, the maximum torque will result when the angle of incidence is normal to the surface and then $i = 0$. It will be also assumed that the center of solar pressure c_{pSR} is located in the furthest possible area of the satellite and c_g is the center of mass of the satellite located in the geometrical center. This gives:

$$\tau_s = F_{SR} \times (c_{pSR} - cg) \tag{4.14}$$

$$\tau_s = 4,51\ 10^{-6} \times (1 + 0,6) \times 0.1^2 \times (0.05 - 0) \tag{4.15}$$

$$\boxed{T_s = 3,645\ 10^{-9}\ \ Nm}$$

4.5 Total Disturbance

In table 4.1 the resulting disturbance torques in their worse-case condition magnitudes are listed.

In order to have total control over the spacecraft, the control system of the CubeSat must be able to produce at least double of this torque [12], so is a value to be used in the reaction wheel sizing.

	Disturbance Torque	**Magnitude [Nm]**
T_g	Gravity Gradient	$7,817\ 10^{-8}$
T_m	Magnetic	$4,702\ 10^{-7}$
T_a	Aerodynamic	$1,330\ 10^{-7}$
T_s	Solar Radiation	$3,645\ 10^{-9}$
T	**TOTAL**	$\mathbf{6,850\ 10^{-7}}$

Table 4.1: Disturbance torques magnitude summary

This resulting total torque value will be also used in the simulation as the applied external torque to the CubeSat. By taking the worst-case condition, we can express the applied external torque vector to the satellite as:

$$T_{ext} = [T_{max} \;\; T_{max} \;\; T_{max}] \tag{4.16}$$

$$T_{ext} = \left[6,850\ 10^{-7} \;\; 6,850\ 10^{-7} \;\; 6,850\ 10^{-7}\right]$$

To understand the variation of the torques' importance depending on the cubesat's orbit altitude, figure 4.1 shows this dependency for LEO and GEO orbits.

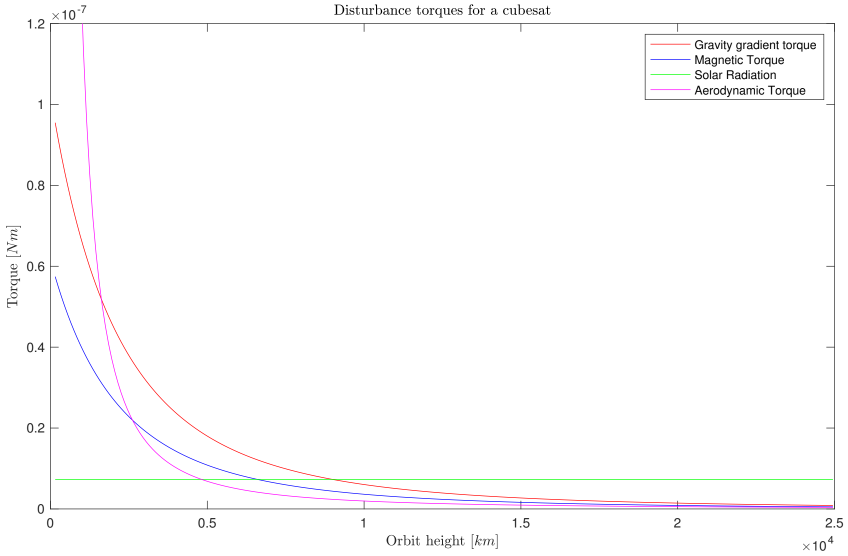

Figure 4.1: Disturbance torques for a CubeSat

As we can see, as our CubeSat orbits at a $h = 300\ km$ LEO orbit, most importance torques are given by Drag, Gravity and Magnetic effects.

Chapter 5

Attitude Control Model Design

5.1 Reaction wheels configurations

The satellite reaction wheel's configuration plays an important role in providing the attitude control torques.

In this section, several configurations based on three or four reaction wheels are investigated in order to identify the most suitable configuration in terms of reliability, time-response and power consumption. To do this, attitude control simulations will be performed for the proposed configurations to get stabilisation time, applied torques and angular velocity performances.

Distribution matrix

In order to find the applied torques in the satellite produced by the reaction wheels, the distribution matrix is to be found for a configuration with more than 3 reaction wheels. In a 4-wheel configuration, we can define it as:

$$T = [t^1 \; t^2 \; t^3 \; t^4] = \begin{bmatrix} r_x^1 & r_x^2 & r_x^3 & r_x^4 \\ r_y^1 & r_y^2 & r_y^3 & r_y^4 \\ r_z^1 & r_z^2 & r_z^3 & r_z^4 \end{bmatrix} \tag{5.1}$$

Where each column vector is a unit vector. According to [6], the distribution matrix in 5.1 satisfies the following equations for each row:

$$r_x^i + r_x^i + r_x^i + r_x^i = 0 \tag{5.2}$$

This implies that in all axes total moment is zero.

5.1.1 Orthogonal 3-wheel configuration

In this configuration, each of the three wheels acts on a single axis as it can be seen in Figure 5.1, thus the distribution matrix results:

$$T = \begin{bmatrix} 1 & 0 & 0 \\ 0 & 1 & 0 \\ 0 & 0 & 1 \end{bmatrix} \tag{5.3}$$

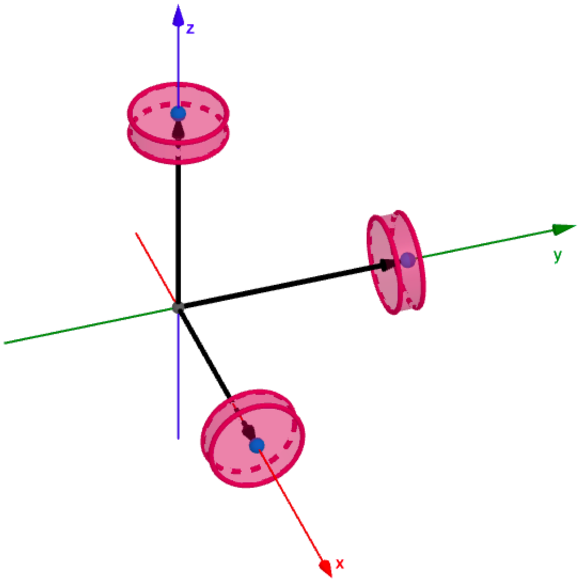

Figure 5.1: Orthogonal 3-wheel configuration

5.1.2 Redundant 4-wheel configuration

As it can be appreciated in figure 5.2, tree wheels are aligned on the primary axis of the satellite as in the previous case, and a redundant wheel has been added tilted at an equal angle from the other wheels. The advantage of this configuration towards the previous one lies in the reliability of the system, as a back-up wheel ensures a longer operative life.

In this case, the distribution matrix can be expressed as:

$$T = \begin{bmatrix} 1 & 0 & 0 & \frac{1}{\sqrt{3}} \\ 0 & 1 & 0 & \frac{1}{\sqrt{3}} \\ 0 & 0 & 1 & \frac{1}{\sqrt{3}} \end{bmatrix} \tag{5.4}$$

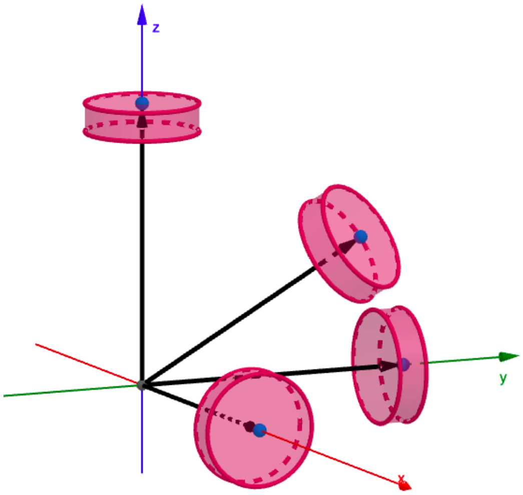

Figure 5.2: Redundant 4-wheel configuration

5.1.3 Tetrahedral 4-wheel configuration

In this configuration, we can also find a fourth wheel redundancy, but here all the wheels have a contribution to the three degrees of freedom, what could lead to a higher resultant torque in the satellite primary axis [6]. This configuration is represented in figure 5.3

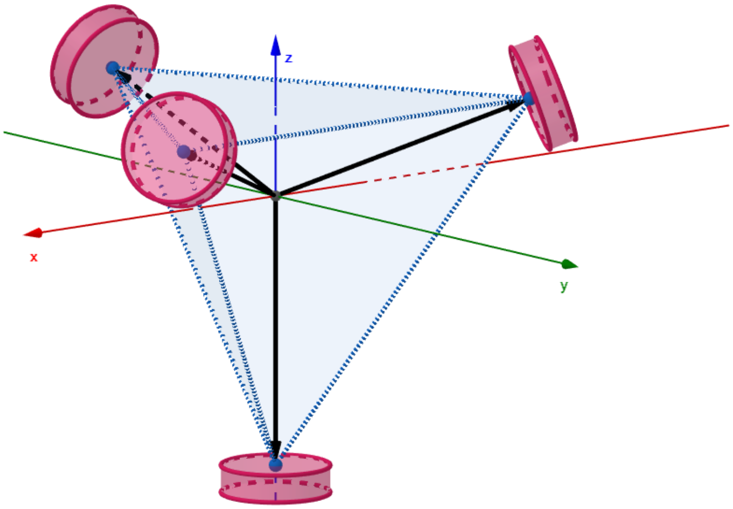

Figure 5.3: Tetrahedron configuration of four reaction wheels

In order to get the distribution matrix of the configuration, some calculations are to be developed. The angle between the actuators in a tetrahedral formation, as it can be seen in figure 5.4 is:

$$\alpha = cos^{-1}\left(-\frac{1}{3}\right) = 109.47^\circ \tag{5.5}$$

In figure 5.3 and 5.4 one possible configuration of the reaction wheels relative to body frame is presented. Wheels 1, 2, 3 present 19.47° angle with $x_b - y_b$ plane. t_1, the first column of T, is placed along the z-axis, then $t_1 = [0\ 0\ -1]$.

Now, from relation in 5.2 we can find that: $r_z^2 = r_z^3 = r_z^4 = 1/3$.

Then, the first approximation becomes:

$$T = \begin{bmatrix} 0 & r_x^2 & r_x^3 & r_x^4 \\ 0 & r_y^2 & r_y^3 & r_y^4 \\ -1 & \frac{1}{3} & \frac{1}{3} & \frac{1}{3} \end{bmatrix} \tag{5.6}$$

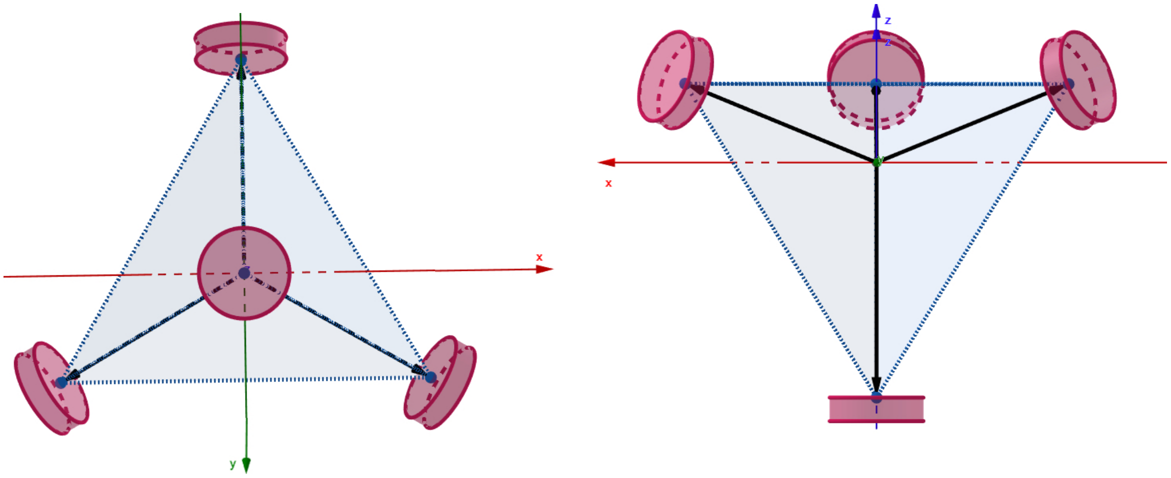

Figure 5.4: Tetrahedron configuration on $x_b - y_b$ and $x_b - z_b$ planes

Now, for finding t_2, $r_x^2 = 0$ is considered and we use the unity vector condition: $\sqrt{0 + (r_y^2)^2 + (1/3)^2} = 1$, results:

$$r_y^2 = \pm\sqrt{1 - (1/3)^2} = \pm\frac{2}{3}\sqrt{2} \tag{5.7}$$

If we choose the negative option $r_y^2 = -\frac{2}{3}\sqrt{2}$, and apply relation 5.2, then $r_y^3 = r_y^4 = \frac{1}{3}\sqrt{2}$.

Finally, applying once again the unity vector condition, we can find t_3 and t_4:

$$\sqrt{(r_x^i)^2 + (1/3\sqrt{2})^2 + (1/3)^2} = 1 \tag{5.8}$$

$$r_x^i = \pm\frac{1}{3}\sqrt{6} \qquad for \quad i = 3, 4 \tag{5.9}$$

And we finally choose $r_x^3 = \frac{1}{3}\sqrt{6}$ and $r_x^4 = -\frac{1}{3}\sqrt{6}$ to find the distribution matrix T:

$$T = \begin{bmatrix} 0 & 0 & \frac{1}{3}\sqrt{6} & -\frac{1}{3}\sqrt{6} \\ 0 & -\frac{2}{3}\sqrt{2} & \frac{1}{3}\sqrt{2} & \frac{1}{3}\sqrt{2} \\ -1 & \frac{1}{3} & \frac{1}{3} & \frac{1}{3} \end{bmatrix} \tag{5.10}$$

5.1.4 Off-centered 4-wheel configuration

In the last 4-wheel configuration that will be presented, all reaction wheels have the same contribution to each of the three primary axes of the satellite.

As it is presented in figures 5.5, the wheels are situated on the four upper octants of the Euclidean three-dimensional coordinate system.

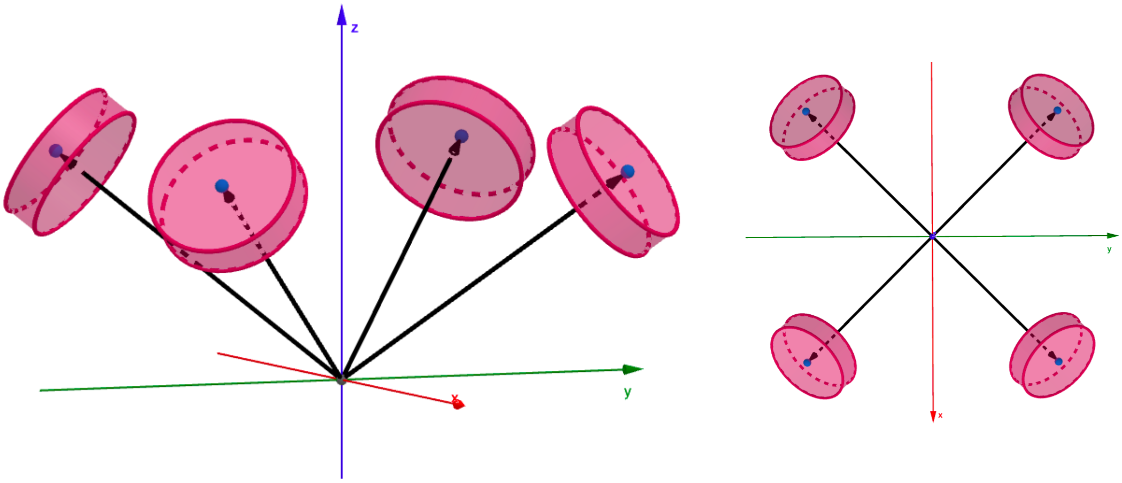

Figure 5.5: Off-centered 4-wheel configuration

Finally, in order to find the distribution matrix, it is only necessary to apply the unity vector condition to the following intuitive matrix:

$$T = \begin{bmatrix} 1 & -1 & -1 & 1 \\ -1 & 1 & -1 & 1 \\ 1 & 1 & 1 & 1 \end{bmatrix} \tag{5.11}$$

And we get:

$$T = \begin{bmatrix} \frac{1}{\sqrt{3}} & \frac{-1}{\sqrt{3}} & \frac{-1}{\sqrt{3}} & \frac{1}{\sqrt{3}} \\ \frac{-1}{\sqrt{3}} & \frac{1}{\sqrt{3}} & \frac{-1}{\sqrt{3}} & \frac{1}{\sqrt{3}} \\ \frac{1}{\sqrt{3}} & \frac{1}{\sqrt{3}} & \frac{1}{\sqrt{3}} & \frac{1}{\sqrt{3}} \end{bmatrix} \tag{5.12}$$

5.2 DC Motor Model

The reaction wheels are driven by motors, in this thesis a brushless DC motor model will be used for the sistem modelisation.

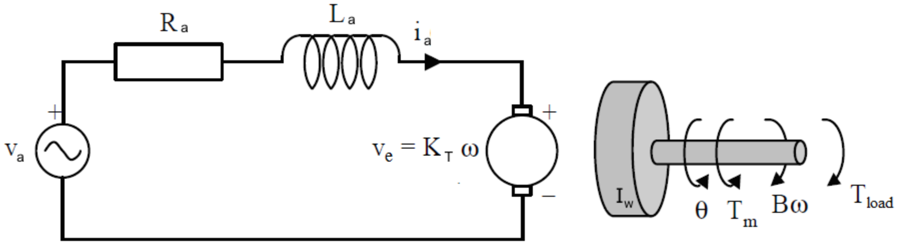

Figure 5.6: DC motor circuit [16]

In image 5.6, the following parameters can be identified:

- $\mathbf{L_a}$: Armature inductance $[H]$
- $\mathbf{R_a}$: Armature resistance $[\Omega]$
- $\mathbf{i_a}$: Input current $[A]$
- $\mathbf{V_a}$: Input voltage $[V]$
- $\mathbf{V_e}$: Input voltage $[V]$
- $\mathbf{K_T}$: Torque constant $[Nm/A]$
- $\mathbf{K_E}$: Field constant $[V/(rad/s)]$
- $\mathbf{T_L}$: Torque load $[Nm]$
- $\mathbf{I_w}$: Reaction wheel inertia $[Kg \cdot m^2]$
- **B**: Rotor friction $[Nm/(rad/s)]$

From the Kirchoff's voltage law for the armature circuit, it derives the following relation:

$$L_a \frac{d}{dt} i_a = -R_a i_a - K_E w_m + u_a \tag{5.13}$$

In a DC motor with constant field, the motor torque is proportional to the armature current [7] and is given by:

$$T = K_T \cdot i_a \tag{5.14}$$

And if we consider that the inertia moment of the motor is negligible in front of the reaction wheel inertia $I_m \ll I_w$, then in order to find the reaction wheel acceleration the rotor friction is to be substracted:

$$T = K_T i_a = I_w \dot{w}_m - Bw \tag{5.15}$$

The block diagram implemented in Simulink is shown in figure 5.7

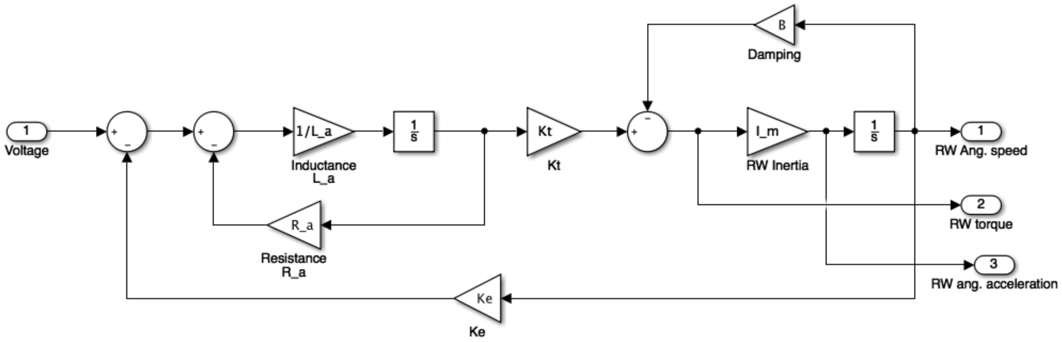
B
Damping
1
Voltage
+
-
+
-
1/L_a
Inductance
L_a
1/s
Kt
Kt
-
+
I_m
RW Inertia
1/s
1
RW Ang. speed
2
RW torque
3
RW ang. acceleration
R_a
Resistance
R_a
Ke
Ke

Figure 5.7: Simulink model of the DC motor

5.3 Commercial Off-The-Shelf Reaction Wheels Assemblies

In order to approximate the Simulations and obtain more accurate results, three commercial Wheel Assemblies are presented and compared. The values in table 5.6 are given for a single wheel. The models described are:

- RW210 Series, from Hyperion Technology [17]
- CubeWheel S, from CubeSpace [18]
- RW 1, from Astro-und Feinwerktechnik Aldershof [19]

The three analysed companies offer 4-wheel assemblies as the one presented in figure 5.9 or single units as in figure 5.8.

	HYPERION TECH. RW210 Series	CUBE SPACE CubeWheel S	ASTROWERKTECHNIK RW 1
Weight (g)	48	60	20
Dimensions (mm)	25 x 25 x 15	28 x 28 x 26.2	21 x 21 x 12
Max speed (rad/s)	15.000	8.000	16.000
Max ct torque (mNm)	0.1	0.23	0.023
Temperature (deg)	-20 to 60	-10 to 60	-20 to 50
Peak power (mW)	630	650	620
Max Voltage (V)	3.5	6.4	5

Table 5.1: Reaction Wheel commercial assemblies

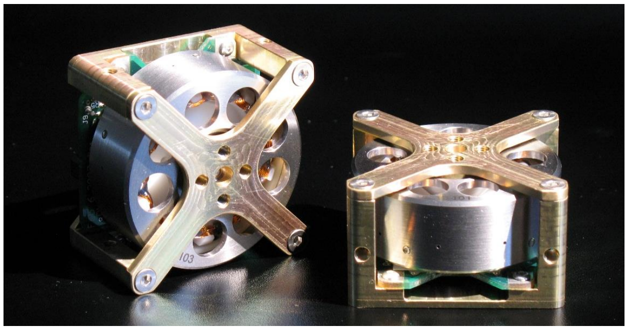

Figure 5.8: Commercial Reaction Wheel

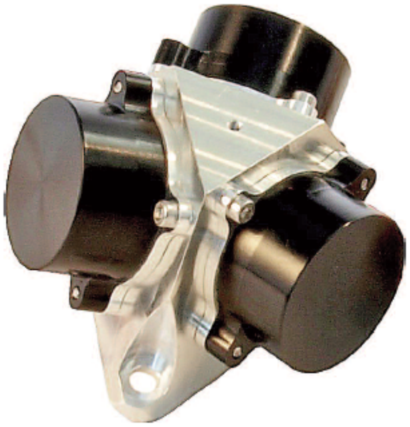

Figure 5.9: Commercial Reaction Wheel Assembly [19]

5.4 The reaction wheels saturation problem

Disturbance torques computed in chapter 4 are continuously applied to the satellite, thus the reaction wheels need to provide constant torque to counter these external torques. As studied in 3, in order to balance the external torques, an angular acceleration of the wheels is required. This angular speed increases the wheels rotational speed over time.

The external torques continuously add energy into the spacecraft, and the wheels accumulate it in angular momentum until reaching a spinning limit. When a wheel reaches this limit it is said to be saturated.

5.4.1 Momentum damping

To prolong the life of a mission there must be a way to expel momentum from the system, otherwise, the spacecraft would lose the attitude control and begin to rotate towards external forces. This is known as momentum damping.

Momentum damping can be done by control jets that fire a thrust in a specific direction in order to relieve the momentum built up on the reaction wheels. This method is commonly used in high orbits or about planets not having enough magnetic field [1]. The complexity of a second system and the problem of a limited propellant source make it a non-desired option for CubeSat and also larger spacecraft.

Magnetic torquers are commonly used in low orbits about planets with an appreciable magnetic field. The main withdraw of this system is the possibility of interference with other components on the spacecraft.

Magnetorquers

A magnetic torque rod is a device based on a electrically conductive wire wrapped around a ferromagnetic rod. When an electric current passes through the coil, it causes the ferromagnetic rod to become magnetic [20] generating a control magnetic dipole, whose intensity can be expressed by:

$$m = nIS \quad \left[Am^2\right] \tag{5.16}$$

Where S is the coil area, n is the number of turns for a simply wounded coil. The magnetic dipole direction is aligned with the coil axes and depends on the current sign. As m is proportional to the supplied electrical current, the produced torque is controllable and can be expressed by:

$$T = m \times B \tag{5.17}$$

Where B is the Earth external magnetic field. As this torque is provided by an external force, the magnetic drag force will be able to take the accumulated energy out of the system.

Finally, it is interesting mentioning that the generated torque vector will be perpendicular both to the coil axis and the external magnetic field vector (see Figure 5.10a. Hence, adding a minimum of 3 perpendicular magnetorquers, the satellite could be fully controlled.

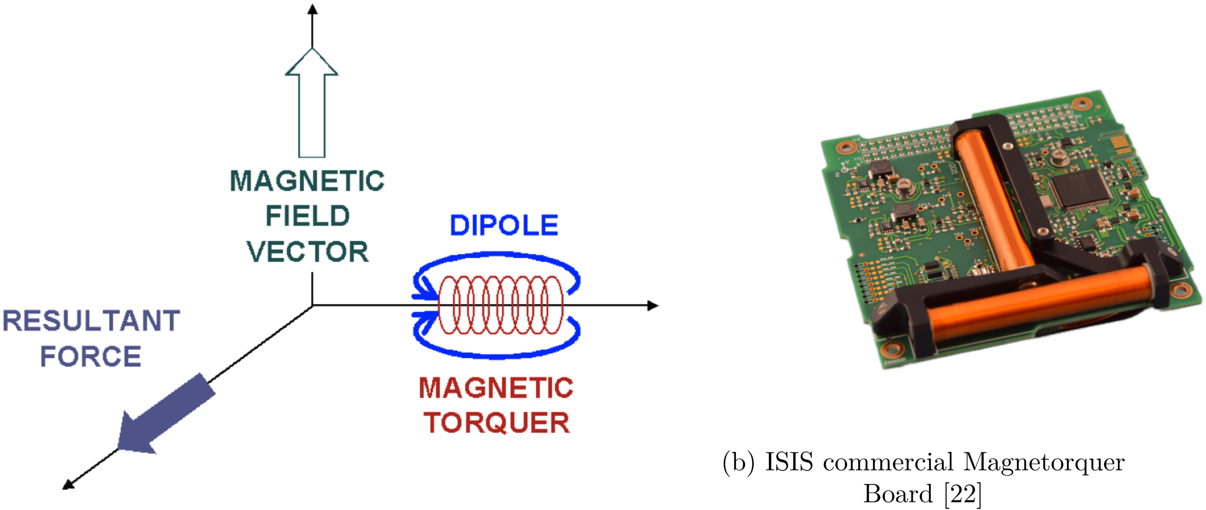

(a) Magnetorquer basic operation principle [21]

(b) ISIS commercial Magnetorquer Board [22]

Figure 5.10: Magnetorquer actuators

In figure 5.10b, a commercial example of magnetorquer board unit suitable for Cubesats is presented.

5.5 Simulink implementation

In this section, the Feedback control in the modelled system is presented. MATLAB Simulink has been used for modelling and simulation.

Following figures show the simplified models developed in Simulink. In Figure 5.11 the model for 3 reaction wheels aligned with the principal axes of the CubeSat is presented. Then, Figure 5.12 shows the model for 4 reaction wheels.

As the 3-wheel model is simpler because the resultant torque of the reaction wheels is already applied into the principle inertia axes of the satellite, the 4-wheel model will be detailed explained hereafter.

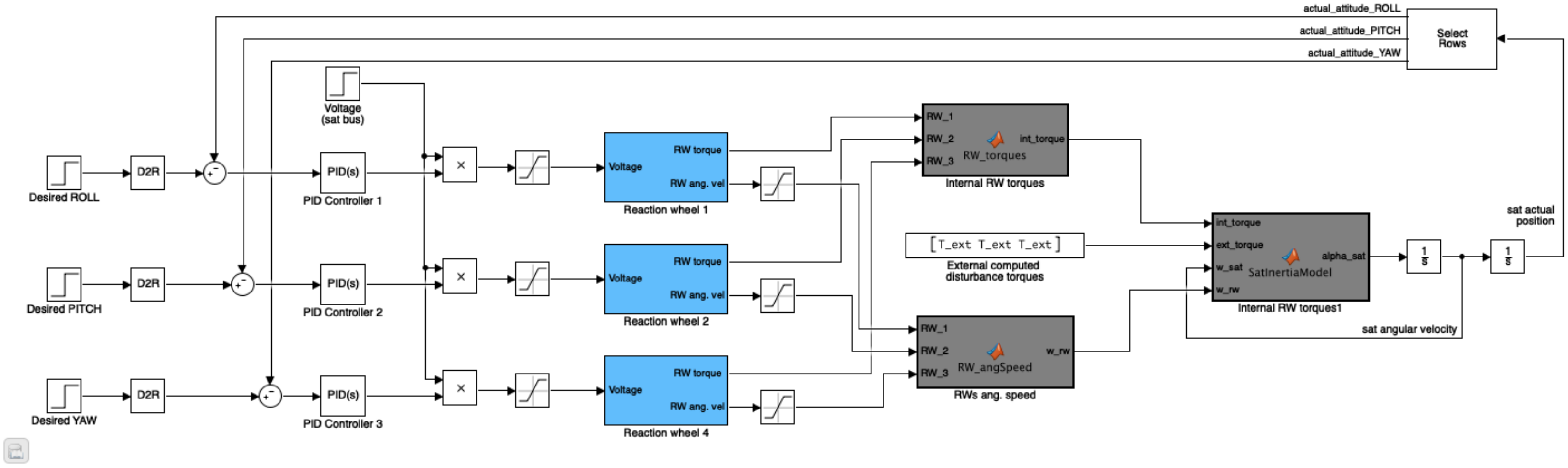
actual_attitude_ROLL
actual_attitude_PITCH
actual_attitude_YAW
Select Rows
Voltage (sat bus)
Desired ROLL
Desired PITCH
Desired YAW
D2R
PID(s)
PID Controller 1
PID Controller 2
PID Controller 3
Voltage
RW torque
RW ang. vel
Reaction wheel 1
Reaction wheel 2
Reaction wheel 4
RW_1
RW_2
RW_3
int_torque
RW_torques
Internal RW torques
[T_ext T_ext T_ext]
External computed disturbance torques
w_rw
RW_angSpeed
RWs ang. speed
int_torque
ext_torque
w_sat
w_rw
alpha_sat
SatInertiaModel
Internal RW torques1
1/s
sat actual position
sat angular velocity

Figure 5.11: Attitude Control System - Simulink model (3-wheels)

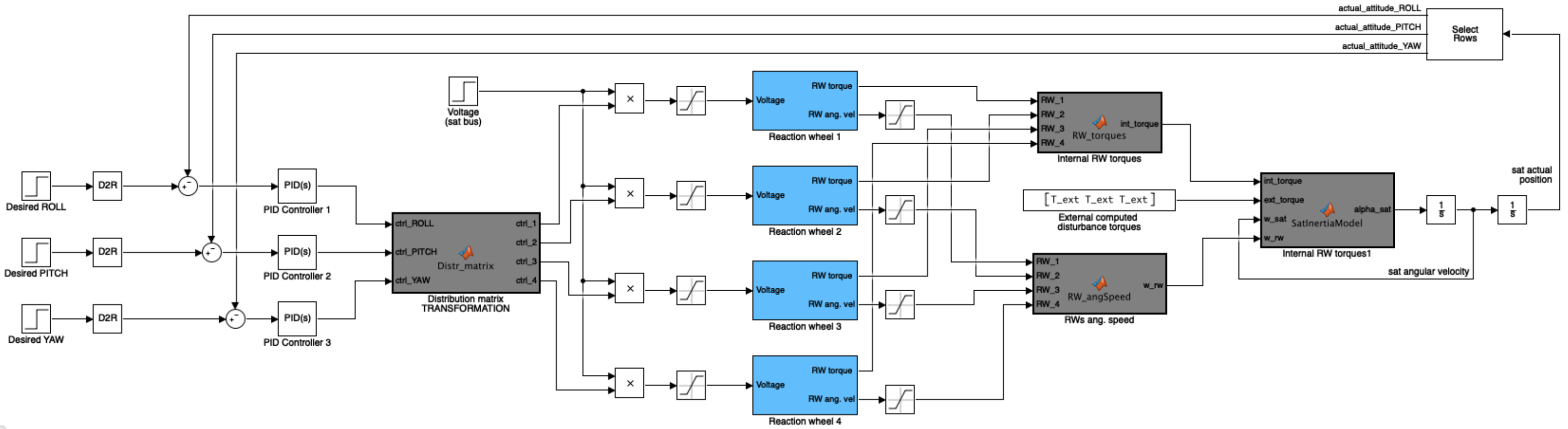
actual_attitude_ROLL
actual_attitude_PITCH
actual_attitude_YAW
Select Rows
sat actual position
Desired ROLL
Desired PITCH
Desired YAW
D2R
D2R
D2R
PID(s)
PID Controller 1
PID(s)
PID Controller 2
PID(s)
PID Controller 3
Voltage (sat bus)
ctrl_ROLL
ctrl_PITCH
ctrl_YAW
Distr_matrix
ctrl_1
ctrl_2
ctrl_3
ctrl_4
Distribution matrix TRANSFORMATION
×
×
×
×
Voltage
RW torque
RW ang. vel
Reaction wheel 1
Voltage
RW torque
RW ang. vel
Reaction wheel 2
Voltage
RW torque
RW ang. vel
Reaction wheel 3
Voltage
RW torque
RW ang. vel
Reaction wheel 4
RW_1
RW_2
RW_3
RW_4
RW_torques
int_torque
Internal RW torques
[T_ext T_ext T_ext]
External computed disturbance torques
RW_1
RW_2
RW_3
RW_4
RW_angSpeed
w_rw
RWs ang. speed
int_torque
ext_torque
w_sat
w_rw
SatInertiaModel
alpha_sat
Internal RW torques1
1/s
1/s
sat angular velocity

Figure 5.12: Attitude Control System - Simulink model (3-wheels)

5.6 Simulink blocks

To start with the simulated satellite attitude control system model, the desired values to achieve are set (in degrees) and will be transformed to radians to afterwards apply the corresponding mechanical and electrical equations.

A typical closed-loop control sequence has been used individually for each degree of freedom as seen in figure 5.13. The PID controllers that define a control command to the system have been tuned for each configuration using the Matlab-Simulink function.

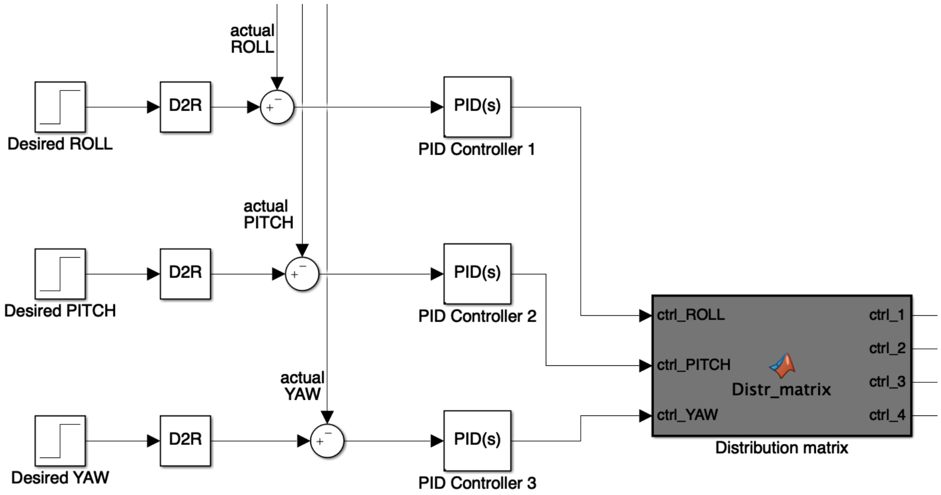
actual ROLL
Desired ROLL
D2R
PID(s)
PID Controller 1
actual PITCH
Desired PITCH
D2R
PID(s)
PID Controller 2
actual YAW
Desired YAW
D2R
PID(s)
PID Controller 3
ctrl_ROLL
ctrl_PITCH
ctrl_YAW
Distr_matrix
ctrl_1
ctrl_2
ctrl_3
ctrl_4
Distribution matrix

Figure 5.13: Simulink model. Control block

The matlab function-block named *Distr_matrix* in Figure 5.13, outputs the control that each reaction wheel has to perform, using the transposed distribution matrix (T^T) defined in section 5.1:

$$\begin{bmatrix} ctr_{\_1} \\ ctr_{\_2} \\ ctr_{\_3} \\ ctr_{\_4} \end{bmatrix} = \begin{bmatrix} r_x^1 & r_y^1 & r_z^1 \\ r_x^2 & r_y^2 & r_z^2 \\ r_x^3 & r_y^3 & r_z^3 \\ r_x^4 & r_y^4 & r_z^4 \end{bmatrix} \begin{bmatrix} ctrl_{\_ROLL} \\ ctrl_{\_PITCH} \\ ctrl_{\_YAW} \end{bmatrix} \tag{5.18}$$

Using the distribution matrix T corresponding to the simulated configuration. The block has as many outputs as actuating reaction wheels.

In Figure 5.14, the satellite control actuators are presented. The Reaction Wheels block diagrams have been explained on previous section 5.2, Figure 5.7.

The control is made by adjusting the voltage provided to the actuators, proportional to the CubeSat voltage bus (a typical value of $6V$ has been used). Then, the voltage is saturated to the maximum allowed by the DC motors (see Table).

Finally, the output reaction wheel velocity is also saturated to $w = 8.000\ rpm$ due to saturation problems as explained in section 5.4

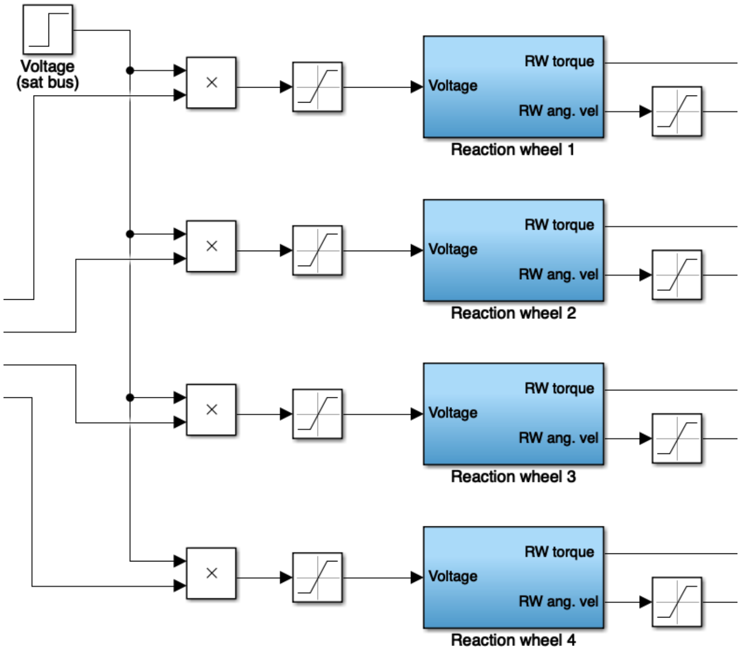
Voltage
(sat bus)
×
Voltage
RW torque
RW ang. vel
Reaction wheel 1
Reaction wheel 2
Reaction wheel 3
Reaction wheel 4

Figure 5.14: Simulink model. Actuators block

Useful values to be used in the satellite attitude dynamics determination are the torque produced by each reaction wheel, and its angular velocity.

The *SatInertiaModel* block implements the following equation from section 3.5:

$$\frac{d\omega_b}{dt} = I^{-1}\left[-\omega_b \times (I\omega_b + h_w) + T_d + T_C\right] \tag{5.19}$$

With h_w being the reaction wheels angular momentum:

$$h_w = TI_w\omega_w \tag{5.20}$$

Which outputs the satellite angular acceleration (*alpha*) using the satellite angular velocity (ω_b), the reaction wheels angular velocity in order to compute h_w (ω_w), the external disturbance torque considered constant (T_d) and the commanded torque produced by the reaction wheels (T_c).

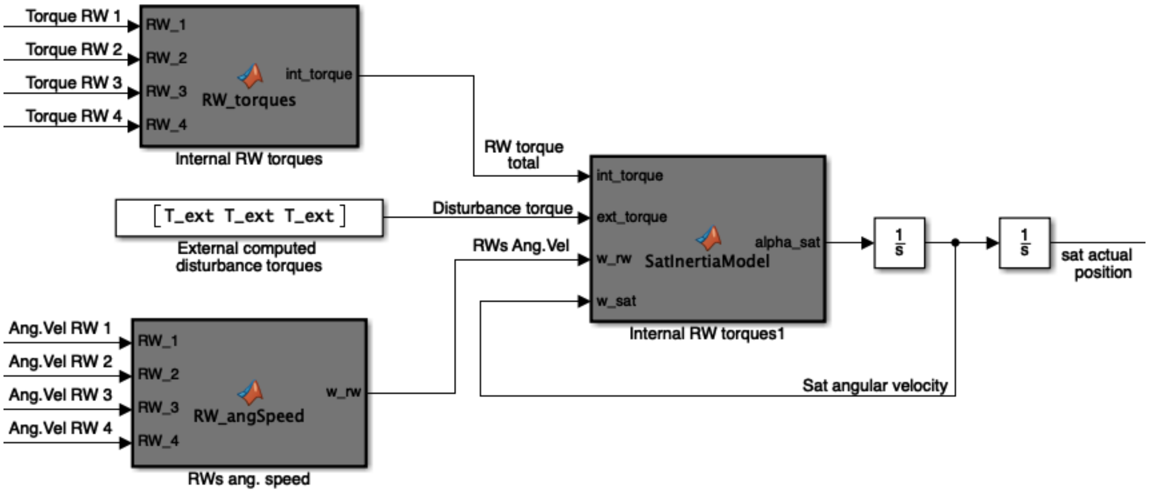
Torque RW 1
Torque RW 2
Torque RW 3
Torque RW 4
RW_1
RW_2
RW_3
RW_4
int_torque
RW_torques
Internal RW torques
RW torque total
[T_ext T_ext T_ext]
External computed disturbance torques
Disturbance torque
RWs Ang.Vel
int_torque
ext_torque
w_rw
w_sat
alpha_sat
SatInertiaModel
Internal RW torques1
1/s
1/s
sat actual position
Sat angular velocity
Ang.Vel RW 1
Ang.Vel RW 2
Ang.Vel RW 3
Ang.Vel RW 4
RW_1
RW_2
RW_3
RW_4
w_rw
RW_angSpeed
RWs ang. speed

Figure 5.15: Simulink model. Attitude dynamics block

The satellite angular acceleration is twice integrated in order to obtain the *actual* angular position that is used in the control loop.

In order to validate the model, a fist scheme in one dimension using one single reaction wheel has been performed and further extended to 3DOFs as the results matched the expected analytical.

Chapter 6

Simulation Results

This chapter treats the Simulink model simulations carried out in order to study the attitude dynamics of a Cubesat based on the model described in previous chapters.

First, different wheels configurations responses are presented in their normal and degraded state -with wheel failures in the redundant configurations. Then, the results obtained are presented in order to take some conclusions.

Simulations have been done using typical CubeSat values:

CUBESAT 1U PARAMETERS

Orbit altitude	h	600	km
Dimensions		$0.1 \times 0.1 \times 0.1$	m
Mass	M	$1,3$	kg
Drag coefficient	C_d	$2,5$	$-$

Table 6.1: Cubesat 1U parameteres

And the actuator parameters correspond to the CubeWheel S from CubeSpace [18] described in section 5.3:

Finally, is also worth mentioning that the full-operative simulations have been performed for the following manoeuvre:

ACTUATOR PARAMETERS

Inductance	L_a	0.48	H
Resistance	R	7	Ω
Motor field ct	K_e	$0.922\ 10^{-3}\ (60/(2\pi))$	$V/(rad/s)$
Motor torque cr	K_t	$8.8\ 10^{-3}\ (60/(2\pi))$	$V/(rad/s)$
Damping coefficient	b	$8.85\ 10^{-6}\ (60/(2\pi))$	$Nm/(rad/s)$
RW mass	m	0.04	kg
RW radius	r	0.028	m
RW heigh	h	0.013	m
Inertia	J_m	$3\ 10^{-6}$	$kg\ m^2$

Table 6.2: Reaction wheels and motor parameters

Degree of Freedom	**Initial**	**Desired**
Roll (ϕ)	0°	180°
Pitch (θ)	0°	90°
Yaw (ψ)	0°	30°

Table 6.3: Defined manoeuvre for the normal-state simulations

6.1 3-wheel configuration

Following figures 6.1, 6.2 and 6.3 present the response of the wheel-configuration presented in section 5.1.1.

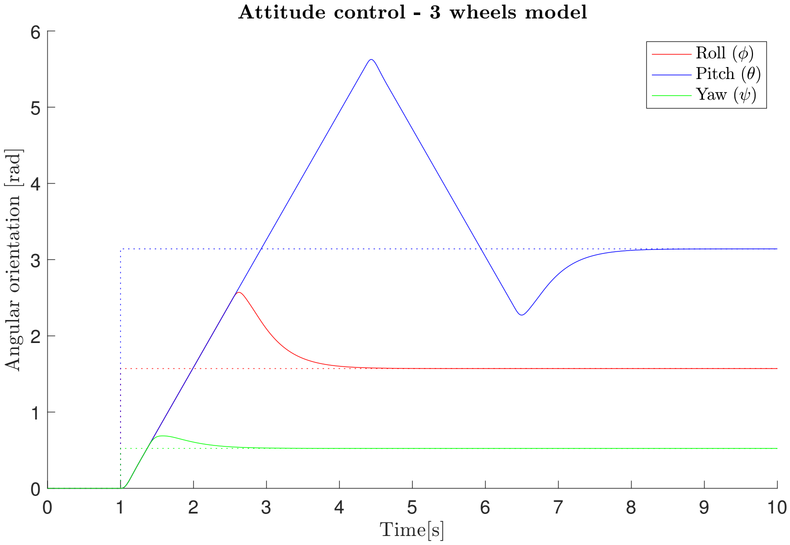

Figure 6.1: Attitude control, 3-wheel configuration

As observed, the CubeSat achieves the desired attitude in $8,03s$, with $20,86J$ energy consumed in the maneuver.

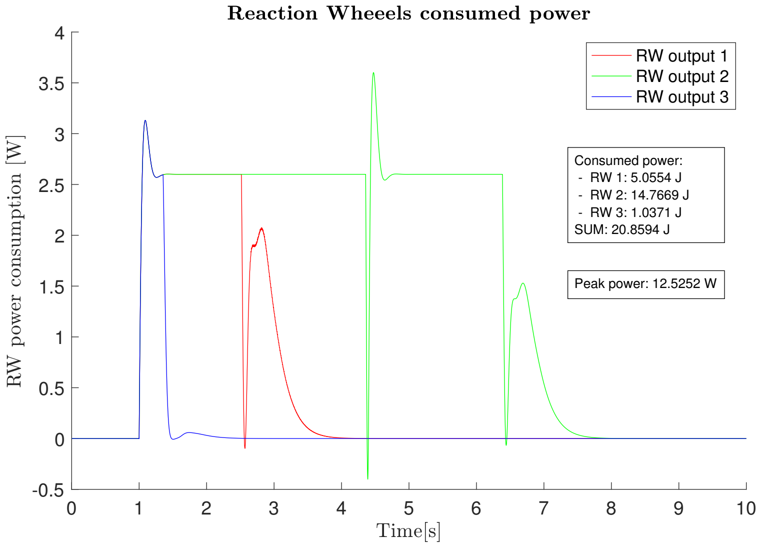

Figure 6.2: Power consumption, 3-wheel configuration

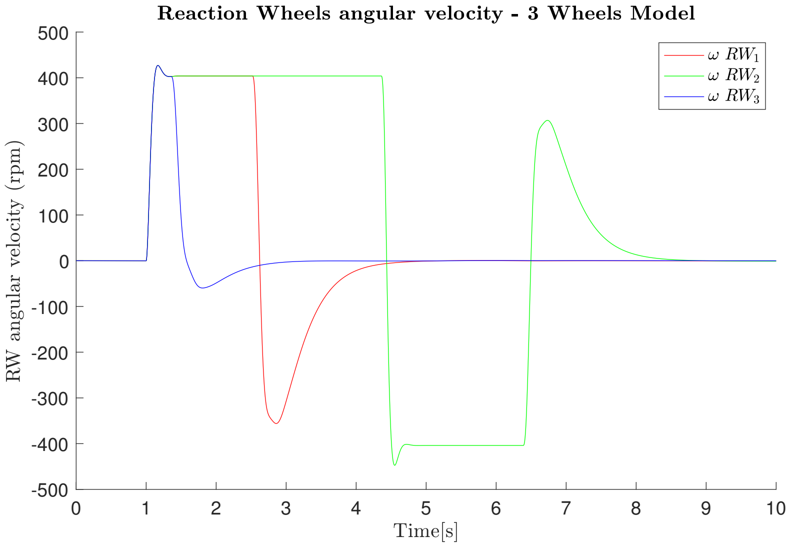

Figure 6.3: Wheels angular velocity, 3-wheel configuration

When the satellite is static and manoeuvre is done, the external torque needs to be countered. To do so, the simulation shows that the higher acceleration on the reaction wheels is constant (as the external applied torque has been considered constant) and results:

$$\alpha \approx 0,16\ rad/s^2 \tag{6.1}$$

This implies that this configuration needs **13h 43m** to arrive to the saturated condition of the wheels spinning at an angular velocity of $\omega > 8.000\ rad/s$

6.2 4-wheel Redundant configuration

Following figures 6.4, 6.5 and 6.6 present the response of the wheel-configuration presented in section 5.1.2.

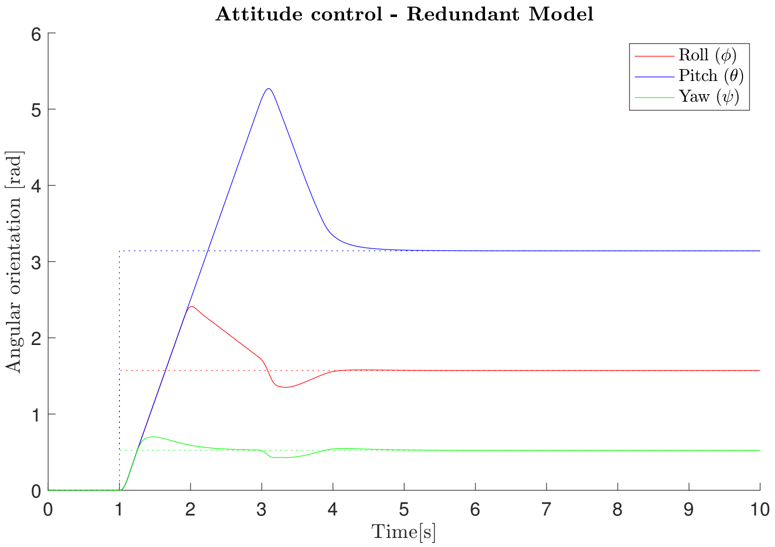

Figure 6.4: Attitude control, 4-wheel Redundant configuration

As observed, the CubeSat achieves the desired attitude in $4,70s$, with $22,87J$ energy consumed in the maneuver.

In this configuration, the higher acceleration on the reaction wheels is a constant value of:

$$\alpha \approx 0,14\ rad/s^2 \tag{6.2}$$

This implies that this configuration needs **15h 50m** to arrive to the saturated condition of the wheels spinning at $\omega > 8.000\ rad/s$

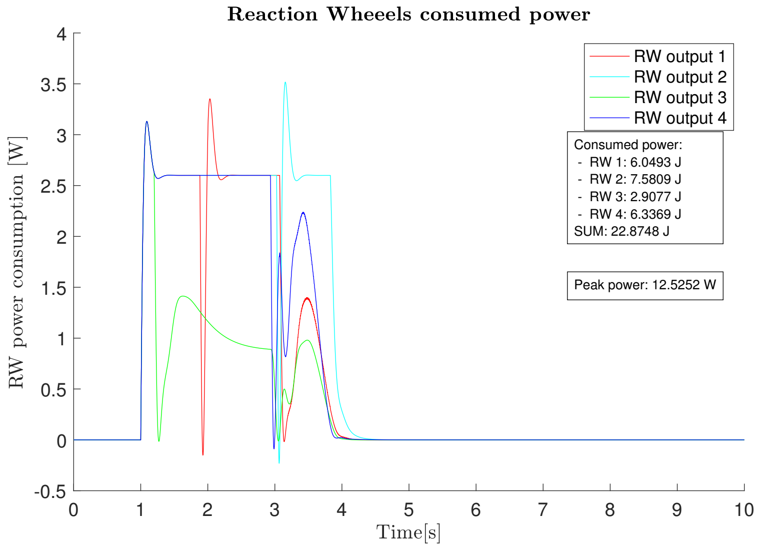

Figure 6.5: Power consumption, 4-wheel Redundant configuration

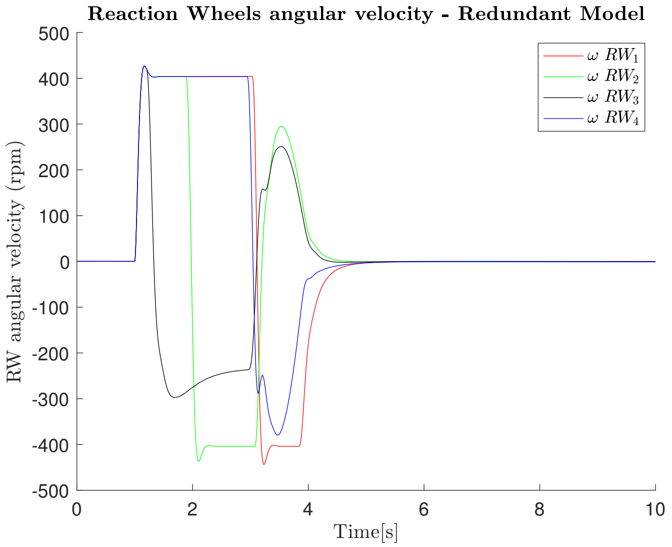

Figure 6.6: Wheels angular velocity, 4-wheel Redundant configuration

6.3 4-wheel tetrahedric configuration

Following figures 6.7, 6.8 and 6.9 present the response of the wheel-configuration presented in section 5.1.3.

As observed, the CubeSat achieves the desired attitude in $4,58s$, with $17,39J$ energy consumed in the maneuver.

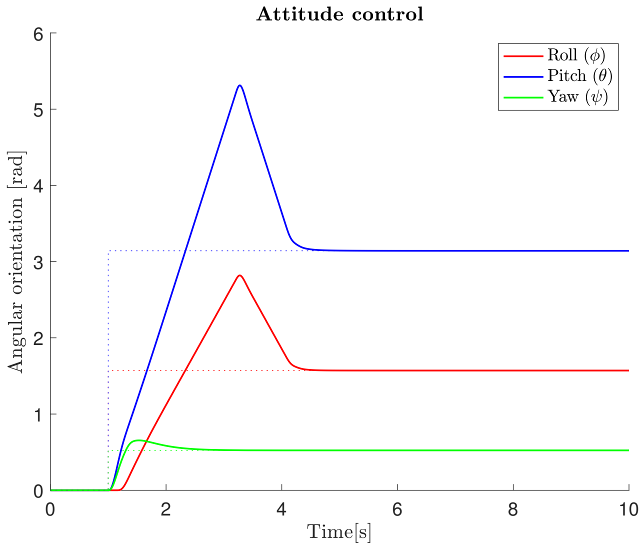

Figure 6.7: Attitude control, 4-wheel tetrahedric configuration

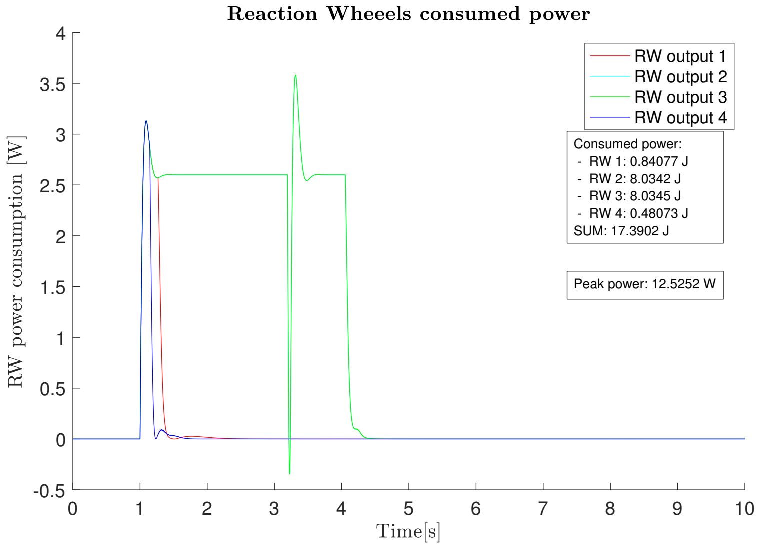

Figure 6.8: Power consumption, 4-wheel tetrahedric configuration

In this configuration, the higher acceleration on the reaction wheels is a constant value of:

$$\alpha \approx 0,19 \; rad/s^2 \tag{6.3}$$

This implies that this configuration needs **11h 17m** to arrive to the saturated condition of the wheels spinning at $\omega > 8.000 \; rad/s$

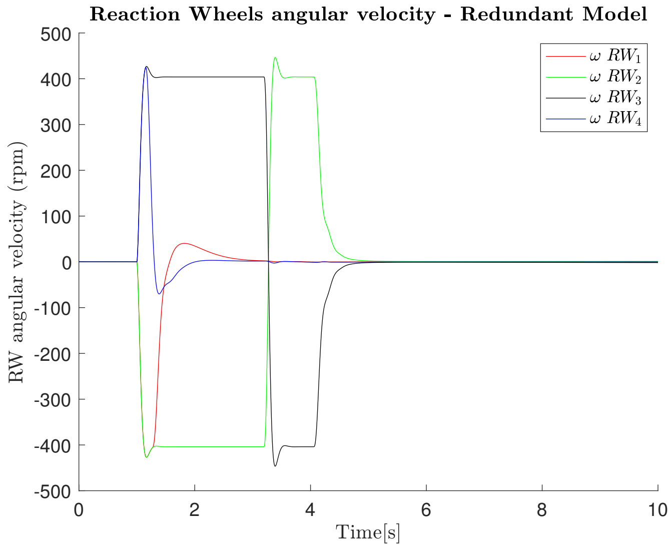

Figure 6.9: Wheels angular velocity, 4-wheel Tetrahedric configuration

6.4 4-wheel Off-centered configuration

Following figures 6.10, 6.11 and 6.12 present the response of the wheel-configuration presented on section 5.1.4.

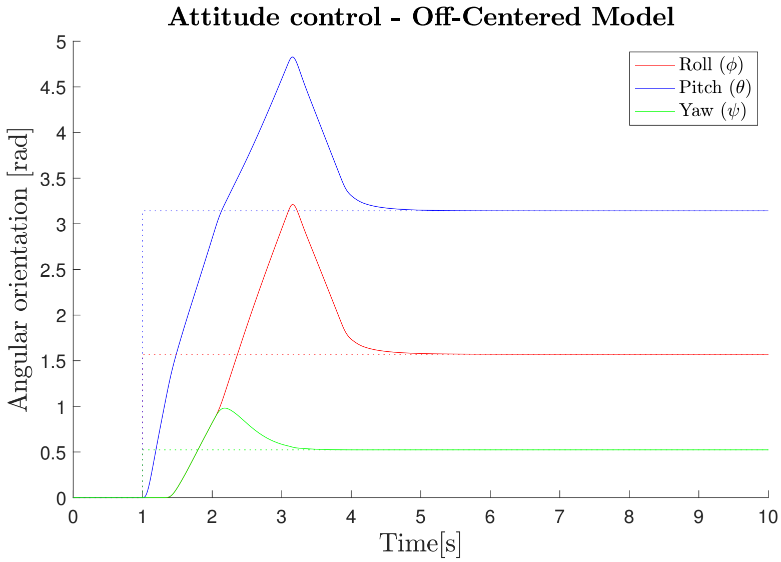

Figure 6.10: Attitude control, 4-wheel Off-centered configuration

As observed, the CubeSat achieves the desired attitude in $4,46s$, with $19,30J$ energy consumed in the maneuver.

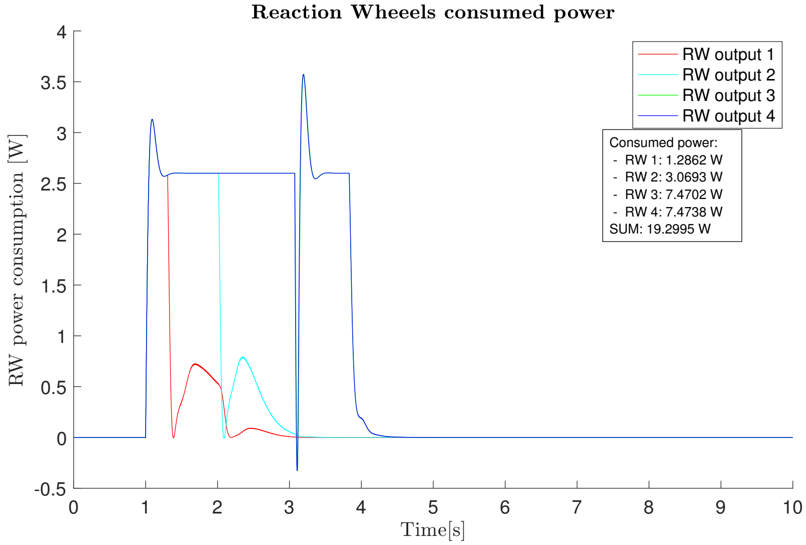

Figure 6.11: Power consumption, 4-wheel Off-centered configuration

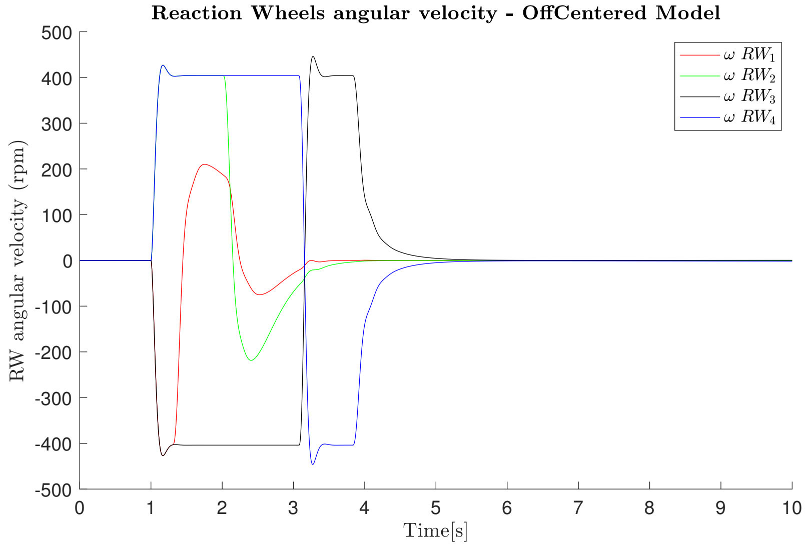

Figure 6.12: Wheels angular velocity, 4-wheel Off-centered configuration

In this configuration, the higher acceleration on the reaction wheels is a constant value of:

$$\alpha \approx 0,21\ rad/s^2 \tag{6.4}$$

This implies that this configuration needs **10h 20m** to arrive to the saturated condition of the wheels spinning at $\omega > 8.000\ rad/s$

6.5 1-wheel failure

The 4 wheels configurations add a redundancy to the system that provides the possibility of a degraded operation in case of a wheel failure.

Here, the plots corresponding to the attitude control in case of one-wheel failure in the three configurations are presented. This degraded-state simulations have been performed for the following manoeuvre (Table 6.4), thanks to being a symmetrical rotation in the three axis, the election of the wheel failure does not spoil the response comparison between configurations:

Degree of Freedom	**Initial**	**Desired**
Roll (ϕ)	0°	30°
Pitch (θ)	0°	30°
Yaw (ψ)	0°	30°

Table 6.4: Defined manoeuvre for the degraded-state simulations

6.5.1 Redundant model failure

For the redundant configuration, two different failure cases are presented as different responses are expected to show up weather the failure comes from one of the axis-aligned wheels or the redundant wheel.

In the case of the redundant-wheel failure, the attitude response is presented in figure 6.13. As it can be observed, the satellite stabilises in a short time and symmetrically in the three axis, as the manoeuvre described in 6.4 is equal in the three degrees of freedom. The failure of this wheel implies a increase of the stabilisation time of a $11,8\%$ with respect to the normal-state for the same manoeuvre.

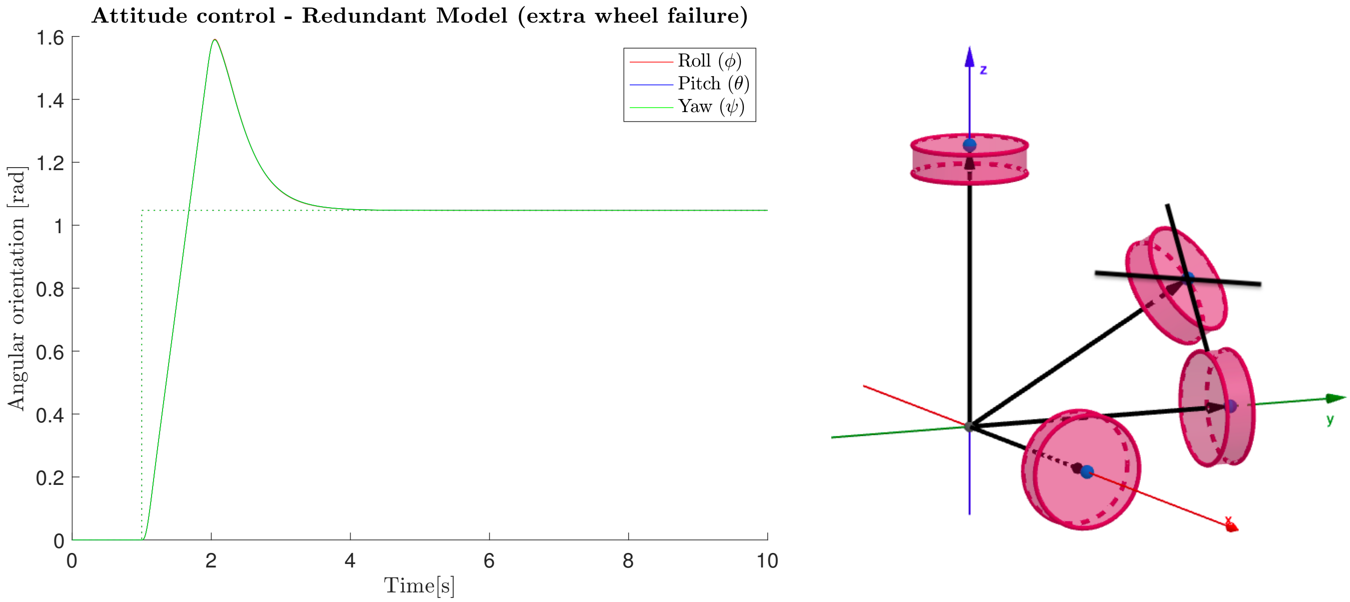

Figure 6.13: Redundant model, extra wheel failure attitude response

Now, another case is presented in which the failure is produced in one of the axis-aligned wheels. The wheel in [0 0 1] has been chosen.

As it can be observed in figure 6.14, the response is much slower $(7,3\ s)$, increasing the stabilisation time of the degraded-mode more than a 90%, and an increase with respect to the normal-state mode of a $114,7\%$

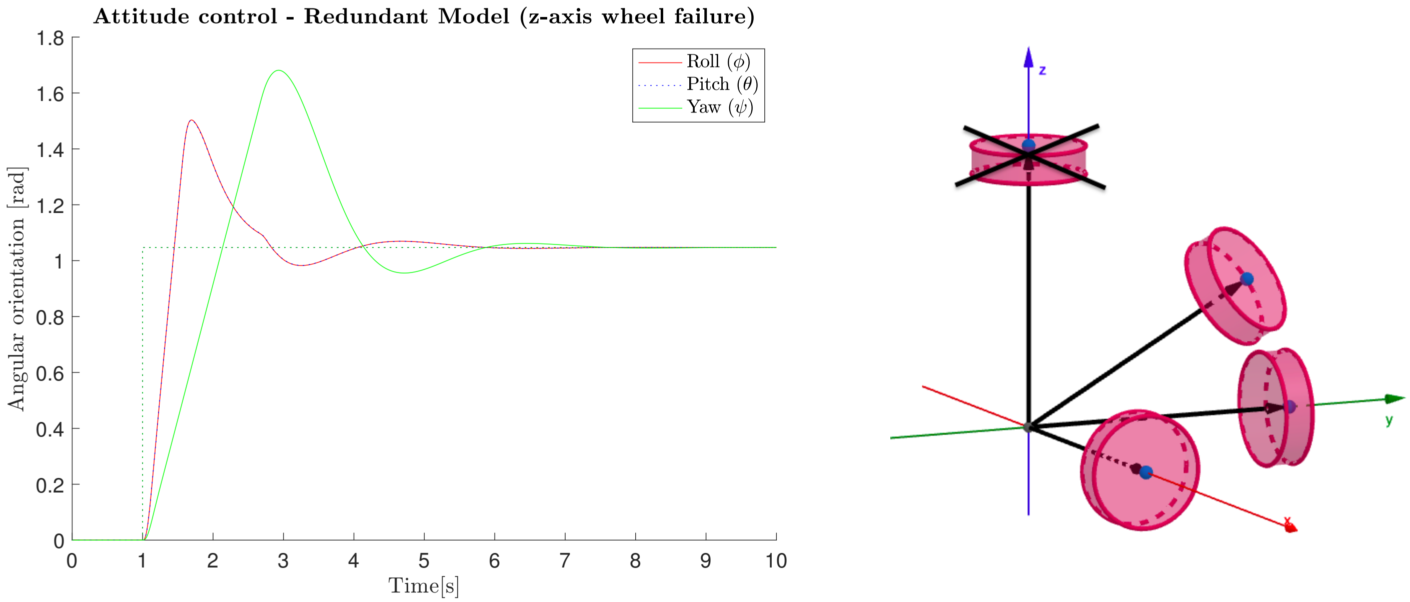

Figure 6.14: Redundant model, z-axis wheel failure attitude response

6.5.2 Off-centered model failure

For the off-centered configuration, the failure of the wheel [1 1 1] has been considered (see Figure 6.15). The attitude reaches the desired value after $5,4\ s$, a value $68,7\%$ higher than the stabilisation time for the same manoeuvre in the normal-mode.

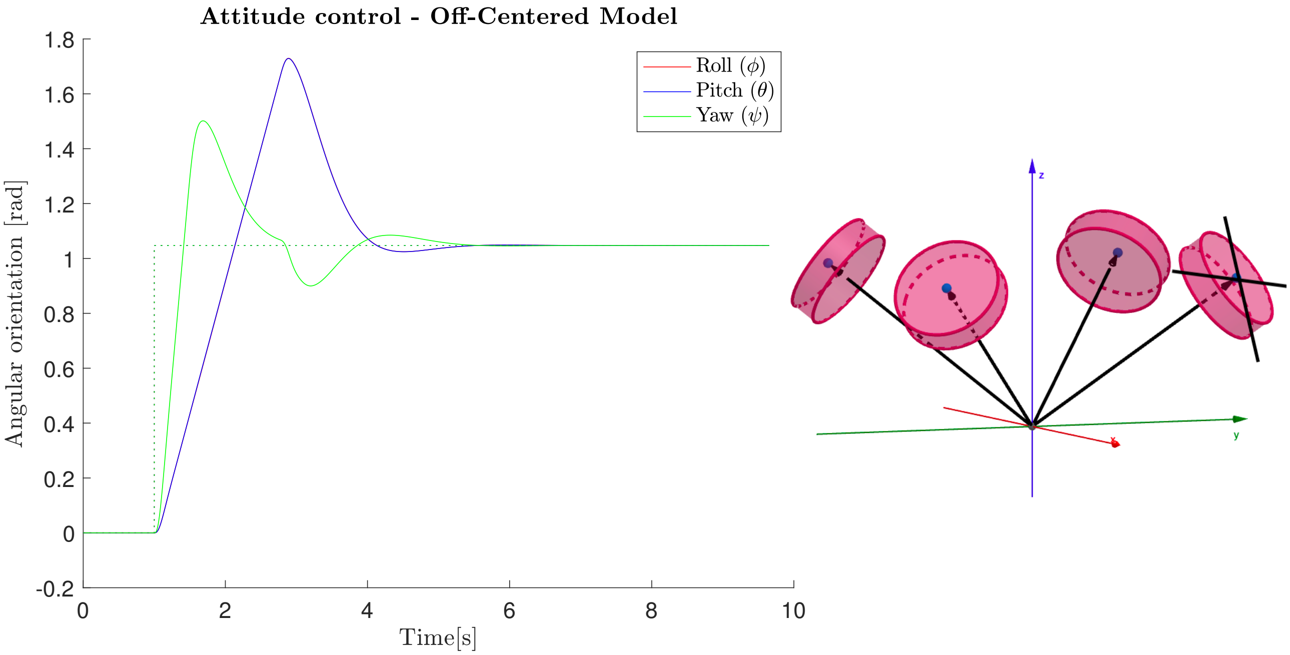

Figure 6.15: Off-Centered model, wheel failure attitude response

6.5.3 Tetrahedric model failure

For the tetrahedric configuration, the failure of the wheel $\begin{bmatrix}-\sqrt{6} & \sqrt{2} & 1\end{bmatrix}$ has been considered (see Figure 6.16). The attitude reaches the desired value after $5,7$ s, a value $78,1\%$ higher than the stabilisation time for the same manoeuvre in the normal-mode.

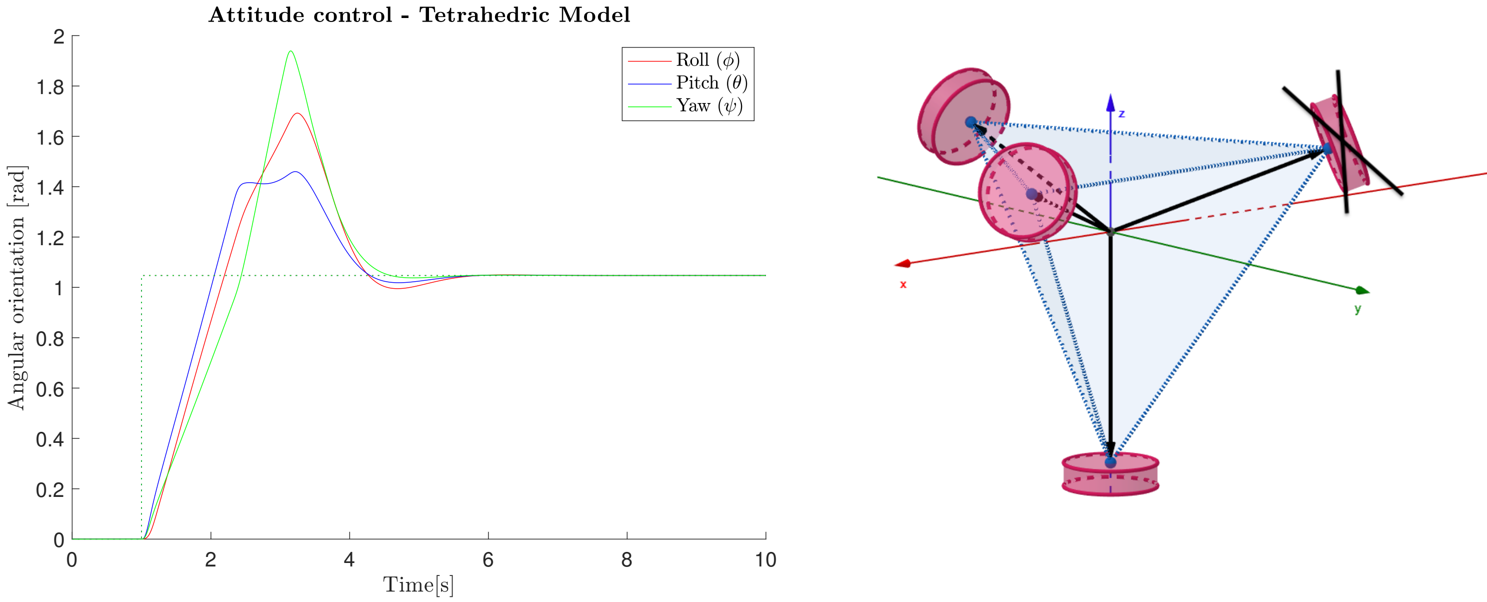

Figure 6.16: Tetrahedric model, wheel failure attitude response

6.6 Comparison

Now is time to analyse the performance of the four configurations. Table 6.5 summarises the most representative values.

		3-wheel	**4-wheel Redundant**	**4-wheel Off-Centered**	**4-wheel Tetrahedric**
Stabilisation time	[s]	8,03	4,7	4,58	4,46
Energy consumed (maneouver)	[J]	20,86	22,87	19,30	17,39
Peak power (maneouver)	[W]	3,6	3,5	3,6	3,6
Max RW vel. (maneouver)	[rad/s]	447	434	446	446
RW acc. (stable state)	[rad/s^2]	0,16	0,14	0,21	0,19
Time to saturate (stable)	-	13h 43m	15h 50m	10h 20m	11h 17m
Failure stabilisation time	[s]	-	7,3 (z-axis) 3,80 (extra)	5,40	5,70

Table 6.5: Reaction wheels configurations performance comparison

The 3-wheel configuration shows up to be less robust, as the resultant torque provided to the satellite cannot be as high as the achieved with a 4-wheel configuration. The advantage of this configuration comes in terms of space and weight added to the satellite, but is clear that a failure in any of the wheels will lead the CubeSat to be uncontrolled and end up its mission time.

The 4-wheel redundant configuration behaves properly with the failure of the redundant wheel, but any other wheel failure reduces its robustness significantly.

The two left configurations (off-centered and tetrahedric) both show up to have very acceptable performances.

Chapter 7

Environmental impact assessment and economical costs

On this chapter, the environmental impact and the economical analysis of the thesis is performed. The environmental analysis includes the resources this project uses, and analyses their impacts on the society and environment [23].

On the economical analysis, a short summary of the budget (see *Budget* attachment) is developed here. The environmental impact of a project like the developed here is very low, taking into consideration the analytic approach - since this thesis does not contemplate any manufacturing process. Hence, the environmental impact analysed on this chapter is limited to the engineering cost.

All the impacts of the project are indirect impacts, since no pollution is generated directly and disposed into the atmosphere and no visual or sound contamination is generated. Therefore, the impact this project has is related directly to the usage of computational resources. These computational resources conventional laptop used for the modelling and simulation of the system. Hence, one has the following table:

Item	**Hours**	**kWh**	**Emission factor [24] [CO_2 kg / kWh]**	**CO_2 Kg**
Computer	350	18	0.385	6.93

Table 7.1: Environmental impact assessment summary

On the economical costs of the project, the following table summarises the several sections taken into account when developing the budget (see *Budget* attachment):

Human Costs	6.600 €
Software Costs	740 €
Hardware Costs	62,5 €
TOTAL COSTS	**7.402, 5€**

Table 7.2: Project's budget summary

Chapter 8

Conclusions

After the three main stages of this thesis: state of the art, system modelling and system simulation, a deeper understanding of an Attitude Control System based on Reaction Wheels is achieved. This comes mostly in terms of space rotating mechanics definition to understand the responses of different reaction wheel configurations.

Respecting the constraints and requirements set by the CubeSat standard and explained at the beginning of the thesis, it is worth mentioning the dimension limitation for a reaction wheel assembly. Reaction wheels are very costly in terms of weight and used space inside the satellite. This is why it is not always a suitable solution and it will depend on the space mission to perform. Moreover, it has been found that saturation problems appear after some operating hours of attitude control and require techniques to attenuate them.

From the simulated reaction wheels configurations, 4-wheel configurations add a redundancy that may be crucial to increase the CubeSat mission time. Then, tetrahedric and off-centred configurations have shown up to perform better than others. Moreover, the attitude control performance achieved is accurate and very fast in time. Hence, reaction wheels are a perfect solution for attitude-depending satellite missions.

8.1 Next steps

On the next steps concerning this study, different Attitude Control techniques can be studied. As having mentioned the reaction wheels saturation problem and proposing magnetorquers as a feasible solution, it is seen that magnetic coils could also be used as a simpler Attitude Control System in the 3 degrees of freedom.

Moreover, the results obtained in this thesis are theoretical and include important simplifications and assumptions. The model could be validated by experimental results for a prototype tested on a test bench in order to determine the roughness of the model and determine further analyses.

Bibliography

[1] Micjhel D. Griffin and James R. French. *Space Vehicle Design.* Second Ed. Blacksburg, Virginia: American Institute of Aeronautics and Astronautics, Inc., 2004.

[2] *CubeSat Design Specification.* Tech. rep. California Polythecnic State University, 2009. URL: `http://www.cubesat.org/images/{\%}0Ddevelopers/cds{\_}rev12.pdf`.

[3] Roger Jove-Casulleras. “Contribution to the Development of pico-satellites for Earth Observation and Technology Demonstrators”. PhD thesis. Universitat Politècnica de Catalunya - BarcelonaTech, 2014.

[4] H. Helvajian and S. Janson. *Small Satellites: Past, Present, and Future.* Tech. rep. Reston, VA, 2009. DOI: `s`.

[5] J. R. Wertz and W. J Larson. *Space mission analysis and design.* Third Ed. Space Technology Library, 1999.

[6] Soner Karatas. “LEO satellites: Dynamic modeling, simulations and some nonlinear attitude control techniques”. PhD thesis. Middle East Technical University, 2006.

[7] Olav Egeland and Jan Tommy Gravdahl. *Modeling and simulation for automatic control.* Norway, 2002.

[8] O. Hegrenes. “Attitude control by means of explicit model predictive control, via multi-parametric quadratic programming”. In: *Department of Engineering Cybernetics, NTNU* (2004).

[9] Jack B. Kuipers. *Quaternions and rotation sequences.* Princeton, New Jersey: Aerospace and Virtual Reality, Princeton University Press, 1999.

[10] Peter C. Hughes. *Spacecraft attitude dynamics.* New York : J. Wiley, 1986, p. 564. ISBN: 0471818429.

[11] J. R. Wertz. *Mission Geometry; Orbit and Constellation Design.* Springer Netherlands, 2001, p. 985.

[12] Charles D. Brown. *Elements of Spacecraft Design.* AIAA (American Institute of Aeronautics and Astronautics), 2002, p. 606.

[13] Jens Giesselmann. "Development of an Active Magnetic Attitude Determination and Control System for Picosatellites on Highly Inclined Circular Low Earth Orbits". PhD thesis. RMIT University, 2006, pp. 1–191.

[14] Eli Jerpseth Øverby. "Attitude control for the Norwegian student satellite nCube". In: *Engineering Cybernetics* (2004), p. 108.

[15] D.A. Vallado and W.D. McClain. *Fundamentals of astrodynamics and applications.* 2001.

[16] Lubica Miková, Ivan Virgala, and Michal Kelemen. "Speed Control of a DC Motor Using PD and PWM Controllers". In: *Solid State Phenomena* Vols. 220- (2015), pp. 244–250.

[17] *Hyperion Technologies.* URL: `https://hyperiontechnologies.nl/products/rw210/` (visited on 08/19/2019).

[18] *CubeSatShop.* URL: `https://www.cubesatshop.com/product/cubewheel-small/` (visited on 08/19/2019).

[19] *Astro-und Feinwerktechnik Aldershof GmbH.* URL: `http://www.astrofein.com/astro-und-feinwerktechnik-adlershof/produkte/` (visited on 08/19/2019).

[20] Isaac Passmore. *Small Satops.* 2018. (Visited on 09/05/2019).

[21] Niccolo Bellini. "Magnetic Actuators for Nanosatellite Attitude Control". PhD thesis. Bologna University, 2014.

[22] ISIS. *ISIS Magnetorquer board.* (Visited on 09/12/2019).

[23] *Ley 21/2013, de 9 de diciembre, de evaluación ambiental.* 2013.

[24] Ministro para la transición Ecológica. *Factores de emisión.* 2019.